Variable-range hopping in quasi-one-dimensional electron crystals

M. M. Fogler

Department of Physics, University of California San Diego, La Jolla, California 92093, USA

S. Teber and B. I. Shklovskii

William I. Fine Theoretical Physics Institute, University of Minnesota, Minneapolis, Minnesota 55455, USA

We study the effect of impurities on the ground state and the low-temperature Ohmic dc transport in a one-dimensional chain and quasi-one-dimensional systems of many parallel chains. We assume that strong interactions impose a short-range periodicity of the electron positions. The long-range order of such an electron crystal (or equivalently, a $4k_F$ charge-density wave) is destroyed by impurities, which act as strong pinning centers. We show that a three-dimensional array of chains behaves differently at large and at small impurity concentrations N. At large N, impurities divide the chains into metallic rods. Additions or removal of electrons from such rods correspond to charge excitations whose density of states exhibits a quadratic Coulomb gap. At low temperatures the conductivity is due to the variable-range hopping of electrons between the rods. It obeys the Efros-Shklovskii (ES) law, $-\ln \sigma \sim (T_{ES}/T)^{1/2}$. T_{ES} decreases as N decreases, which leads to an exponential growth of σ. When N is small, the metallic-rod (also known as "interrupted-strand") picture of the ground state survives only in the form of rare clusters of atypically short rods. They are the source of low-energy charge excitations. In the bulk of the crystal the charge excitations are gapped and the electron crystal is pinned collectively. A strongly anisotropic screening of the Coulomb potential produces an unconventional linear in energy Coulomb gap and an unusual law of the variable-range hopping conductivity $-\ln \sigma \sim (T_1/T)^{2/5}$. The parameter T_1 remains constant over a finite range of impurity concentrations. At smaller N the 2/5 law is replaced by the Mott law, $-\ln \sigma \sim (T_M/T)^{1/4}$. In the Mott regime the conductivity gets suppressed as N goes down. Thus, the overall dependence of σ on N is nonmonotonic. In the case of a single chain, the metallic-rod picture applies at all N. The low-temperature conductivity obeys the ES law, with log corrections, and decreases exponentially with N. Our theory provides a qualitative explanation for the transport properties of organic charge-density wave compounds of TCNQ family.

I. INTRODUCTION

In recent years electron transport in quasi-one-dimensional (quasi-1D) systems moved into focus of both fundamental and applied research. Quantum wires, nanotube ropes, conducting molecules, etc., are being examined as possible elements of miniature electronics devices. In parallel, discovery of quasi-1D structures termed "stripes" in correlated electron systems (high-T_c cuprates, quantum Hall devices, etc.), invigorates efforts to understand unconventional phases in two and three dimensions starting from models of weakly coupled 1D chains.

Experimentally, the low-temperature conductivity $\sigma(T)$ of quasi-1D systems is often of the insulating type. Its temperature dependence gives information about the nature of charge excitations. For example, the activated dependence $-\ln \sigma(T) \propto 1/T$ indicates a gap in the spectrum. In quasi-1D systems such a gap commonly arises from the Mott-Peierls mechanism,[1,2] where the commensurability with the host lattice is crucial. Yet there are many 1D and quasi-1D systems where commensurability plays a negligible role. In this situation the jellium model (an electron gas on a positive compensating background) is a good approximation. This is the kind of systems we study in this paper. We will show that their low-temperature transport is dominated by a variable-range hopping (VRH), which leads to a slower than exponential T dependence[3,4] of the conductivity. Our theory may

apply to a number of systems, both naturally occurring and man-made. Prototypical 1D examples are individual quantum wires on carbon nanotubes. Stripe phases,[5,6] quantum wire arrays in heterojunctions,[7] carbon nanotube films,[8] and atomic wires on silicon surface,[9] are two-dimensional (2D) examples. In three dimensions (3D), an important and well studied class of quasi-1D compounds is charge-density waves[10–12] (CDW).

To characterize the strength of Coulomb correlations in a quasi-1D system we define the dimensionless parameter $r_s \equiv a/2a_B$, where a is the average distance between electrons along the chain direction and $a_B = \hbar^2 \kappa / m e^2$ is the effective Bohr radius. The latter is expressed in terms of the dielectric constant of the medium κ and the electron band mass m. In practically all known realizations of 1D and quasi-1D systems, r_s exceeds unity, often by orders of magnitude. Below we assume that $r_s \gg 1$. Under this condition the dynamics of electrons can be treated semiclassically. Neglecting quantum fluctuations altogether for a moment, we arrive at the picture of electrons forming a classical 1D Wigner crystal in the case of a single chain [Fig. 1(a)] or an array of such crystals in 2D and 3D [Figs. 1(b) and (c)], with the period along the chain equal to a. Formation of the crystal enables the electrons to minimize the energy of their mutual Coulomb repulsion. In order to correctly assess the role of quantum fluctuations (zero-point motion) in such crystals, one has to take into account two circumstances. First is the unavoidable presence
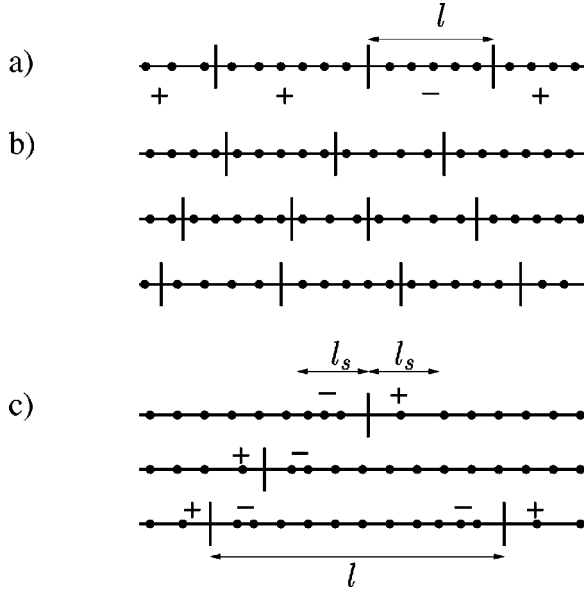
FIG. 1. Pinned 1D and quasi-1D systems on a uniformly charged positive background. Dots and tick marks label the positions of electrons and impurities, respectively. (a) 1D crystal. The $+$ and $-$ signs denote the charge of the metallic rods, which have an average length of l. (b) An array of decoupled chains in the case $l < l_s$. (c) An array of coupled chains for the case $l > l_s$. The preferred arrangement of the electrons on neighboring chains may depend on the exact geometry of the system. In order not to complicate the drawing, we adopted the convention where the ground state corresponds to the same horizontal positions of electrons on each chain. The interchain interactions try to diminish the deviations from this ground state leading to dipolar distortions of a characteristic length l_s around impurities.

of random impurities that act as pinning centers. Second is a finite interchain coupling (in 2D and 3D systems). Either one is sufficient to make the quantum fluctuations of electron positions bounded. For example, in the case of a single chain, the slow growth of the zero-point motion amplitude with distance[13,14] is terminated at the nearest strong pinning center. In higher dimensions, the zero-point motion amplitude is finite even without impurities because of the interchain interaction. In fact, renormalization-group approaches[15] indicate that the Wigner crystal or, equivalently, $4k_F$ CDW is the true ground state of a system of weakly coupled chains starting already from rather modest r_s. In all situations, the net effect of quantum fluctuations is to slightly renormalize the bare impurity strength and/or bare interchain coupling. The calculation of renormalized parameters is possible via the standard bosonization technique.[16] For the treatment of, e.g., 1D case, one can consult Refs. 13,14,17 and 18. Below such a renormalization is assumed to be taken into account and it is not discussed further. Henceforth we will often refer to the systems we study as *electron crystals*.

Due to impurity pinning, at zero temperature and in the limit of small electric field (Ohmic regime) the conductivity of the electron crystal vanishes. This behavior is common for all pinned systems. It motivated a large body of work[19,12] devoted to mechanisms of *nonlinear* transport that become

possible in the presence of a finite electric field, in particular, creep and sliding. In the present context, such mechanisms would involve a collective motion of large numbers of electrons that overcome pinning barriers either by thermal activation or by quantum tunneling. It has been understood, however, on some qualitative level,[19] that if compact charge excitations are allowed by the topology of the system, then such excitations would dominate the response at low temperatures and would give rise to a nonzero *Ohmic* conductivity at $T > 0$. Below we will demonstrate that this is indeed the case in the electron crystals. We clarify the nature of the compact low-energy charge excitations and propose a theory of their low-temperature Ohmic transport that consistently addresses the role of long-range Coulomb interactions.[20]

In this paper we are focused exclusively on the charge transport and ignore any effects related to the spin degree of freedom. This is legitimate for $r_s \gg 1$ because electron are tightly localized at the sites of the classical Wigner crystal and the energy of their spin-dependent exchange interaction is exponentially small.

We will assume that impurities that pin the crystal are strong enough to enforce preferred order of electrons nearby or, in the CDW terminology, the preferred phase. The relation between the phase ϕ and the elastic displacement of the crystal u is $\phi = -(2\pi/a)u$. In Fig. 1 impurities are shown by vertical tick marks and it is assumed that they interact with nearby electrons by a repulsive potential comparable in magnitude to the Coulomb interaction energy $e^2/\kappa a$ between nearest electrons on the chain. This condition is sufficient to ensure that the impurity to act as a strong pinning center. An example of such an impurity is an acceptor residing on the chain. In the ground state one electron is bound to the acceptor and the electron-acceptor complex (of total charge e) is built into the crystal, i.e., it is positioned squarely in between the two closest other electrons. One can say that the crystal contains a plastic deformation—a vacancy bound to the negatively charged acceptor. Overall, the region around the impurity is electrically neutral.

In the case of a single chain [Fig. 1(a)], strong impurities divide the crystal into segments, which behave as individual metallic rods. A charge can easily spread over the length of each rod, while it has to tunnel through an impurity to move to a neighboring rod. Each rod contains an integer number of electrons but the charge of the positive background is random because of the assumed incommensurability. In the ground state the distribution of the rods' total charges, electrons plus background, is uniform between $-e/2$ and $+e/2$ (ϕ is between $-\pi$ and π). Larger charges cost more Coulomb energy and correspond to charge excitations above the ground state. Transitions between ground and excited states occur by discrete changes in the number of electrons on the rods.

Let ε be the minimal by absolute value change in the self-energy of a given rod due to change of its charge by one unit. By the self-energy we mean the Coulomb energy of interaction among the electrons on the given rod, charges on all other rods held fixed. We adopt the convention that the chemical potential (Fermi energy) corresponds to the zero energy. In this case, ε is non-negative (nonpositive) for ad-

dition (subtraction) of the electron. We denote by $g_B(\varepsilon)$ the distribution function of ε averaged over impurity positions. We refer to g_B as the bare density of states of charge excitations. In Sec. III we show that random distribution of charges of the rods creates a finite $g_B(0)$. Small ε come from rods with net charges close to $\pm e/2$. These rods make possible a VRH conductivity at low temperatures.

Consider now a 3D system of parallel chains. Impurities with concentration N divide the chains into segments of average length $l = 1/Na_\perp^2$, where $a_\perp^2$ is the area per chain in y-z plane (we assume the chains to be along the x direction). We get two cases distinguished by the relative importance of interchain interactions. In the first case [Fig. 1(b)], the chains are far enough from each other and/or the impurity concentration is large enough so that the interchain coupling over the length $\sim l$ of a typical segment can be neglected in comparison with its longitudinal compression energy. As a result, the phases of different segments are uncorrelated and the system again behaves as a collection of metallic rods. Polarizability of the rods generates a strongly anisotropic dielectric constant. Like for a single chain, in the ground state of the system, a finite bare density of states g_B at zero energy originates from random background charges of the rods. Again this leads to the VRH at low temperatures.

In the other case [Fig. 1(c)], the concentration of impurities is small and chains are strongly interlocked. The elastic distortions are concentrated in small regions around individual impurities (see below). Away from impurities the crystal possesses a good 3D order. The true long-range order is however absent because of the cumulative effect of small elastic distortions in a large volume. The elastic displacement field $\bar{u}(\mathbf{r})$ of the electron crystal lattice away from impurities gradually varies in space. The length scale where its variation is of the order of a (variation in ϕ is of the order of unity) is referred to as Larkin length. The Larkin length is exponentially large,[21,22] effectively infinite, because the Coulomb interactions make the crystal very rigid. This will be discussed in more detail in Sec. V.

The region near a typical impurity has the following structure.[23] On one side of the impurity the chain is compressed, which creates an excess negative charge; on the opposite side, it is stretched resulting in a positive charge of the same absolute value $\leqslant e/2$. The net charge of such a dipole is zero (together with the vacancy of charge $-e$ and the acceptor of charge e). The characteristic length of the distorted region is of the same order as the length l_s of the nonlinear topological excitation[24–26] of the pure system, the 2π soliton. This is because the magnitude of local distortions in ϕ are typically comparable in the two cases. The formal definition of l_s is[27]

$$l_s = a_\perp/\sqrt{\alpha}, \qquad (1)$$

where $\alpha = Y_\perp/Y_x \ll 1$ is the dimensionless anisotropy parameter and Y_x and $Y_\perp$ are the longitudinal and transverse elastic moduli of the electron crystal. The elasticity theory of the crystal will be discussed in more detail in Sec. V. Here we just mention that α varies from material to material, e.g., α

$\sim 10^{-4}$ in $K_2Pt(CN)_4Br_{0.3}*3(H_2O)$ (KCP) and in CDW organics, $\alpha \sim 10^{-2}$ in blue bronze.[10,11]

At low temperatures all solitons are bound to acceptors with large binding energies comparable to the creation energy of a free soliton $W \sim e^2/\kappa l_s$. In other words, there is a large energy gap for creating charge excitations. Nevertheless, as shown in Sec. V, finite g_B at zero energy does exist in the case $l \gg l_s$ as well. It comes from rare clusters of several closely spaced impurities. Such clusters can be viewed as microscopic inclusions of the $l \ll l_s$ phase (where g_B is large).

In all cases outlined above, g_B is not yet the actual density of states of charge excitations. This is because the long-range Coulomb interaction of charges at distant sites is not included in the definition of g_B. We denote the true density of states of charge excitations by $g(\varepsilon)$. Based on previous studies of other insulating systems, such as doped semiconductors,[28,4] we expect that long-range interactions generate a Coulomb gap in $g(\varepsilon)$. This gap is soft, in the sense that $g(\varepsilon)$ vanishes only at the Fermi level $\varepsilon = 0$. Away from the Fermi level, $g(\varepsilon)$ increases in a power-law fashion until it saturates at the bare value g_B at large enough ε (cf. Ref. 4 and Fig. 10.4 therein). Note that g is different from the thermodynamical density of states. The latter does not vanish despite Coulomb correlations, see Refs. 4 and 29.

In macroscopically *isotropic* electron systems the functional form of the Coulomb gap depends on the number of dimensions. The density of states behaves as ε^2 in 3D and as $|\varepsilon|$ in 2D. In all dimensions, however, this leads to the ES law for the VRH conductivity in isotropic doped semiconductors,[28,4]

$$\sigma = \sigma_0 \exp[-(T_{ES}/T)^{1/2}], \qquad (2)$$

where σ_0 is a prefactor, which has an algebraic T dependence. Parameter T_{ES} is given by

$$T_{ES} = Ce^2/\kappa\xi, \qquad (3)$$

where ξ is the (isotropic) decay length of localized electron states, κ is the (isotropic) dielectric constant of the semiconductor, and C is a numerical coefficient. (We measure temperature in energy units throughout this paper.) In lightly doped isotropic semiconductors κ and ξ are determined solely by material parameters (binding energy of impurity states, electron effective mass, band structure, etc.). Therefore, T_{ES} does not depend on the impurity concentration and Eqs. (2) and (3) are in this sense universal.

In contrast, in this paper we show that in strongly *anisotropic* systems the Coulomb gap has, in general, a different functional form. Depending on l and other parameters, it may be either universal or not [i.e., $g(\varepsilon)$ and T_{ES} may contain factors related to impurity concentration]. These results and their consequences for the VRH transport are presented in the following section.

II. RESULTS

We group our results in the following three sections according to the three cases outlined in the Introduction.

A. Single chain

In this case, studied in Sec. III, the Coulomb interaction is not screened. However, in 1D the $1/x$ decay of the Coulomb potential is on the borderline between the short- and the long-range interactions. Consequently, most physical quantities differ from their counterparts for the short-range (screened) interaction only by some logarithmic factors. For example, the density of states of charge excitations exhibits a logarithmic suppression,[30]

$$g(\varepsilon) = \frac{g_B}{\ln(e^2/\kappa l |\varepsilon|)}. \tag{4}$$

In a first approximation, such a suppression can be disregarded in the calculation of the VRH transport, namely, one can assume that $g(\varepsilon) = g_B = \text{const}$. In this approximation one arrives at the conventional Mott VRH,[3,28] which in 1D coincides with the ES law of Eq. (2). Let us denote by $T_{ES}^{(0)}$ the value of T_{ES} that one obtains neglecting the Coulomb gap, then $T_{ES}^{(0)} \sim 1/g_B \xi_x$. Here ξ_x stands for the localization length that determines the asymptotic decay $P \propto \exp(-2x/\xi_x)$ of the probability of tunneling of charge-e excitations over a large distance x. If the probability of tunneling between nearest rods is written in the form $\exp(-2s)$, where $s \gg 1$, then tunneling paths with returns can be neglected. In this case $\xi_x = l/s$. Using the expression for s from Ref. 13, we obtain

$$\xi_x \sim \frac{l}{r_s^{1/2} \ln^{3/2}(l/a)}, \tag{5}$$

$$T_{ES}^{(0)} = C_1 \frac{e^2}{\kappa l} r_s^{1/2} \ln^{5/2}(l/a). \tag{6}$$

In the last equation we absorbed numerical factors into the coefficient $C_1 \sim 1$.

A similar expression for $T_{ES}^{(0)}$ was obtained by Nattermann et al.[31] for the model of a disordered Luttinger liquid with short-range interactions and weak pinning. Our Eqs. (5) and (6) differ from the corresponding results of Ref. 31 by two logarithmic factors. One of them originates from logarithmic charging energy of metallic rod; the other, from the logarithm in the tunneling action s, see also Refs. 13, 18, and 32.

Once the logarithmic Coulomb gap is taken into account, the T dependence of the conductivity can still be written in the form of an ES law [Eq. (2)] but T_{ES} becomes a function of T, as follows:

$$T_{ES} = T_{ES}^{(0)} \ln \left(\frac{e^2}{\kappa l T_{ES}^{(0)}} \sqrt{\frac{T_{ES}^{(0)}}{T}} \right). \tag{7}$$

Note that in the 1D case, the standard derivation[3] of the VRH law (2) overlooks the role of very resistive hops in some exponentially rare places along the chain. A more careful approach shows[33,32] that Eq. (2) and its generalization through Eq. (7) are valid *only if the chain is sufficiently short*. The quantitative criterion on the length of the chain

can be obtained following the excellent discussion in Refs. 33 and 32. This, however, goes beyond the scope of the present work.

B. 3D systems with large impurity concentrations

This case, formally defined by the inequality $a_\perp \ll l \ll l_s$ is studied in Sec. IV. It may be realized in strongly anisotropic CDW compounds such as KCP where the soliton length l_s is large ($10^2 a$ or so) and/or in samples where a relatively high impurity concentration is created intentionally[34,35] so that l is small. Possible non-CDW realizations include arrays of relatively distant 1D conductors, e.g., quantum wires, nanotubes,[36] or polymers.[37]

As elaborated in Sec. I, impurities divide the system into a collection of metallic rods. The finite 3D concentration of highly polarizable rods results in a large dielectric constant[38] along the x axis. The Coulomb interaction is therefore strongly anisotropic but the Coulomb gap remains parabolic, $g(\varepsilon) \propto \varepsilon^2$, as in isotropic systems. Tunneling is anisotropic as well. The interchain tunneling is accomplished by single-electron-like excitations, which do not perturb charges on the intermediate chains along the tunneling path. In Appendix B we estimate the corresponding transverse localization length $\xi_\perp$ to be

$$\xi_\perp = \frac{a_\perp}{\ln(e^2/\kappa a t_\perp)}, \tag{8}$$

where $t_\perp$ is the interchain hopping matrix element in the tight-binding band-structure model. For the low-T VRH conductivity we again obtain the ES law with T_{ES} given by

$$T_{ES} = C_2 \frac{e^2}{\kappa l} \left[\frac{a_\perp^2 \sqrt{r_s}}{\xi_\perp^2} \ln \left(\frac{l}{a_\perp} \right) \right]^{1/3}. \tag{9}$$

Here C_2 is another numerical factor of the order of unity. We see that in both Secs. II A and II B, the ES law looses its universality, because T_{ES} depends on the impurity concentration N through $l = 1/Na_\perp^2$. For a single chain (Sec. II A) this dependence originates mainly from the dependence of the localization length ξ_x on l. In 3D (case B), the full effective dielectric constant and therefore, the density of states inside the Coulomb gap depend on N as well. In both cases, with decreasing N the temperature T_{ES} decreases, which at a fixed temperature leads to an exponentially increasing conductivity.

In doped semiconductors similar violations of the universality of Eq. (2) are known to occur near the metal-insulator transition. In that case, however, T_{ES} has an *opposite* dependence on N. In particular, T_{ES} vanishes when N grows and reaches the critical concentration.[4] Similarly, previous theories of the VRH transport in strongly anisotropic systems dealt with gapped, semiconductorlike materials (commensurate CDW) where impurities provided carriers,[39,40] so that the conductivity was found to *grow* with the impurity concentration. In contrast, our work is devoted to systems,
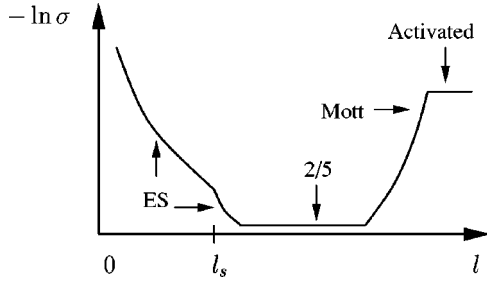
FIG. 2. Logarithm of the resistivity as a function of the average interimpurity distance $l = 1/Na_\perp^2$ at a fixed temperature $T \ll W$. The ES, 2/5, Mott, and activation laws succeed each other with growing l.

which are metallic (sliding) in the absence of impurities. Therefore, decrease of T_{ES} with decreasing N seems natural.[39,40]

At high temperatures, the conductivity is due to the nearest-neighbor hopping. Its T-dependence is of activated type,

$$\sigma = \sigma_A \exp(-E_A/T), \quad l < l_s, \tag{10}$$

with the activation energy

$$E_A \sim \frac{e^2}{\kappa l} \tag{11}$$

and the prefactor σ_A proportional to the probability of tunneling between adjacent rods.

C. 3D systems with small impurity concentration

As impurity concentration decreases and l becomes larger than l_s, a number of dramatic changes appear in all key quantities, such as the density of states, the localization length, and the effective dielectric constant. For example, as we discuss in Sec. V, the dielectric constant starts to increase exponentially with l because the polarizability of the crystal with $l > l_s$ becomes limited not by the length l of individual chain segments but by the exponentially large length of Larkin domains. The soaring dielectric constant causes a rapid drop of the ES parameter T_{ES}. In turn, this causes a collapse of the low-temperature resistivity in a narrow interval $l_s \lesssim l \lesssim l_s \ln(W/T)$ (see the descending branch of the curve in Fig. 2). Until this point, the notion that our system is opposite to the conventional semiconductors, so that purer samples have higher conductivities, seems to be working.

Once l exceeds $l_s \ln(W/T)$, the Larkin length L_x can be treated as effectively infinite. The VRH now involves hops between low-energy states separated by distances shorter than L_x. On such distances, the dispersion of the dielectric function becomes important. Each pair of low-energy charge excitations localized on their respective impurity clusters interacts via a strongly anisotropic electrostatic potential, which is not exponentially small only if the vector that connects the two charges is nearly parallel to the chain direction. Such an unusual interaction leads to a Coulomb gap that is linear in energy and independent of N, unlike the previous case (Sec. II B, $l \ll l_s$), where the Coulomb gap is quadratic

and N dependent. Another difference from Sec. II B is that the localization length ξ_x for the tunneling in the chain direction is also independent of N,

$$\xi_x \sim \frac{l_s}{\sqrt{r_s}}, \tag{12}$$

see Sec. V and Appendix B. This leads to a 2/5 law for the VRH conductivity

$$\sigma = \sigma_0 \exp[-(T_1/T)^{2/5}], \tag{13}$$

where parameter T_1, given by

$$T_1 = C_3 \frac{e^2 r_s^{1/4}}{\kappa l_s} \frac{a_\perp}{\xi_x}, \tag{14}$$

does not depend on l and is, in this sense, universal. Here C_3 is yet another numerical coefficient of the order of unity. The 2/5 law shows up as an intermediate resistivity plateau in Fig. 2. This universal law for quasi-1D systems with $l \gg l_s$ is an analog of the universal ES law in isotropic systems.

We show in Sec. V that the Coulomb gap affects mainly a finite-energy interval $|\varepsilon| \lesssim \Delta$, where $\Delta \propto g_B$ can be called the Coulomb gap width. At larger energies, the density of states of charge excitations coincides with the bare one, $g(\varepsilon) \simeq g_B$. Since g_B is generated by impurity clusters whose concentration diminishes with growing l, both g_B and Δ decrease with l. Eventually, the Coulomb gap becomes more narrow than the range of energies around the Fermi level responsible for hopping at given T. At this point the Coulomb gap can be neglected and the 2/5 law is replaced by the conventional Mott law

$$\sigma = \sigma_0 \exp[-(T_M/T)^{1/4}], \tag{15}$$

where $T_M = C_4/g_B \xi_x \xi_\perp^2$, $C_4 \sim 1$. As l increases further, T being fixed, σ decreases because of diminishing g_B. This gives rise to the ascending branch in Fig. 2. At such l, the electron crystal behaves similar to a gapped insulator where a lower impurity concentration corresponds to a lower carrier density, and thus, to a higher resistivity.

As l continues to grow, at some point the Mott VRH crosses over to the nearest-neighbor hopping and shortly after it becomes smaller than the conductivity due to thermally activated free solitons,

$$\sigma = \sigma_A \exp(-W/T). \tag{16}$$

At even larger l, σ ceases to depend on l, and so the impurity concentration, see Fig. 2. Note that the activation energies $W \sim e^2/\kappa l_s$ [Eq. (16)] and $E_A \sim e^2/\kappa l$ [Eq. (11)] in Secs. II A and II B, respectively, smoothly match at $l \sim l_s$.

D. Summary of the regimes

The rich behavior of the conductivity as a function of l and T is summarized in the form of a regime diagram in Fig. 3. The 2/5 law applies in a broad range of l and T between the ES and the Mott laws.

A convenient way to keep track of all the VRH exponents derived in this paper is provided by Eq. (17) below. We
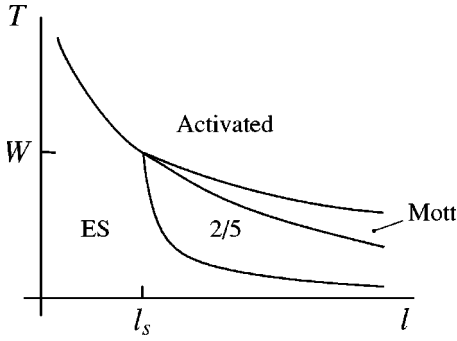
FIG. 3. Summary diagram for the transport regimes in a 3D system. Domains of validity of ES [Eq. (2)], Mott [Eq. (15)], activated [Eqs. (10), and (16)] and 2/5 [Eq. (13)] laws are shown.

would like to present it in a somewhat more general form, motivated by the following physical reasoning.

The diagram of Fig. 3 is obtained under the assumption that the tunneling in the transverse direction is not negligible ($\xi_\perp$ is not too small), so that the VRH has a 3D character. However, if the conducting chains are relatively distant from each other either along y or z direction or both, this condition may be violated. Examples of such systems are artificial arrays of quantum wires[7] and carbon nanotubes.[8] In those systems, the 3D hopping is pushed to very lower temperatures, while at intermediate T the hopping can be either one or two dimensional. Generalizing the standard derivation of the VRH transport[3,4] to the d-dimensional hopping and a power-law density of states $g(\varepsilon) \propto \varepsilon^\mu$, one obtains the conductivity in the form

$$\sigma = \sigma_0 \exp[-(T_{\text{VRH}}/T)^\lambda], \quad \lambda = \frac{\mu+1}{\mu+d+1}. \quad (17)$$

For $d=3$ one recovers all the regimes discussed prior in this section (Mott, 2/5, and ES laws) by setting μ successively to 0, 1, and 2, according to the physical situation. For the sake of completeness, the exponents for other d's in the same situations are summarized in Table I. Inclusion of all such regimes would transform Fig. 3 into a more complicated diagram, but would not change its general structure, so it will not be shown here or discussed further below.

III. 1D SYSTEM

In the case of a single chain of electrons on a uniform positive background [Fig. 1(a)] impurities divide the 1D electron crystal in separate pieces, which behave as metallic

TABLE I. The exponents λ of VRH conductivity [Eq. (17)] in the cases of 3D, 2D, and 1D tunneling and a power-law dependent density of states $g(\varepsilon)$ that arises due to 3D Coulomb interactions. 1D tunneling corresponds to $\xi_\perp \rightarrow 0$.

Tunneling	$g = \text{const}$	$g \propto |\varepsilon|$	$g \propto \varepsilon^2$
3D	1/4	2/5	1/2
2D	1/3	1/2	3/5
1D	1/2	2/3	3/4

rods. The rod lengths x are distributed randomly around the average value l. Therefore, the background charge of a given rod, $Q = -ex/a$, is a random number. It can be written as $Q = -e(n+\nu)$, where n is an integer and ν is a number uniformly distributed in the interval $-1/2 < \nu < 1/2$.

In the ground state of the system each rod contains an integer number n_r of electrons, so that the rod has the total charge of $q = e(n_r - n - \nu)$. To find n we use the fact that the Coulomb self-energy of the rod is equal to $q^2/2C_r$, where $C_r = \kappa x/[2 \ln(x/a)]$ is the capacitance of this rod. On the other hand, the interaction of different rods does not contain the large logarithm $\ln(x/a)$, and can be neglected in the first approximation. Thus, the minimization of the total energy of the system amounts to minimizing the self-energies of the rods. One can show then that, in the ground state, $n_r = n$, so that the charges of the rods are uniformly distributed in the interval $-e/2 < q < e/2$. Indeed, if this is not true and the charge of the given rod is $q > e/2$, then, by charge conjugation symmetry, there should exist another rod with the same length and the opposite charge $-q$. Transferring an electron from the first rod to the second one we lower the total energy and make the absolute values of both charges smaller than $e/2$.

Below we use $q = -e\nu$ and call rods with $0 < \nu < 1/2$ empty and with $-1/2 < \nu < 0$ occupied. We define the energy of an empty state, $\varepsilon(x, \nu)$, as the minimum work necessary to bring to it an electron from a distant pure 1D electron crystal with the same average linear density of electrons

$$\varepsilon(x, \nu) = \frac{e^2}{\kappa x} \ln\left(\frac{x}{a}\right) [(1-\nu)^2 - \nu^2] = \frac{e^2}{\kappa x} \ln\left(\frac{x}{a}\right)(1-2\nu). \quad (18)$$

This energy is positive and vanishes only at $\nu = 1/2$. On the other hand, the energy of an occupied state is defined as minus the maximum work necessary to extract electron from this rod to the same distant pure 1D electron crystal. In this case the final result is identical to Eq. (18) with $\nu \rightarrow -\nu$. Apparently, states with $|\nu| = 1/2$ are exactly at the Fermi level, which we take as the energy reference point (it coincides with the electron chemical potential of a pure 1D crystal). The low-energy states relevant to VRH transport have $|\nu| - 1/2 \ll 1$.

Now we can calculate the density of such states. Taking into account the fact that this rod length x is distributed according to Poisson statistics, the disorder-averaged bare density of states can be written as

$$g_B(E) = \frac{1}{l} \int_0^{1/2} d\nu \int_0^\infty \frac{dx}{l} \exp\left(-\frac{x}{l}\right) \delta(E - \varepsilon(x, \nu)). \quad (19)$$

With a logarithmic accuracy, we can replace $\ln(x/a)$ by $\ln(l/a)$. Then we use Eqs. (18) and (19) to find

$$g_B(\varepsilon) = \frac{1}{2\varepsilon_0 l} \left[1 - \left(1 + \frac{\varepsilon_0}{\varepsilon}\right) \exp\left(-\frac{\varepsilon_0}{\varepsilon}\right)\right], \quad (20)$$

where $\varepsilon_0 = e^2 \ln(l/a)/\kappa l$. We warn the reader that one should not attribute much significance to the predictions of the

above formula in the region of high energies, $\varepsilon \gtrsim \varepsilon_0$, where excitations with charges larger than e will also contribute to various physical processes. On the other hand, close to the Fermi level, for $\varepsilon \ll \varepsilon_0$, only charge-$e$ excitations are important, in which case Eq. (20) is fully adequate, while g_B is nearly constant,

$$g_B \simeq \frac{\kappa}{2e^2 \ln(l/a)}. \qquad (21)$$

For the calculation of the low-T transport, only this constant value is needed.

As mentioned in Sec. II, in 1D the $(1/x)$-Coulomb interaction creates only marginal effects on the conductivity. If we neglect them, in the first approximation, then standard Mott's argument[3] leads to the VRH that obeys the $T^{1/2}$ law, Eq. (2), with $T_{ES} = T_M = C_1/g_B \xi_x$, where ξ_x is localization length for tunneling between distant rods. The value of ξ_x is obtained from the following considerations. Tunneling through an impurity that separates two adjacent rods can be viewed as a process in imaginary time that consists of the following sequence of events.[32] A unit charge assembles into a compact soliton just before the impurity in one rod, tunnels through the impurity, and finally spreads uniformly over the other rod. We assume that the chain is not screened by external metallic gates. Then the tunneling probability can be written in the form $\exp(-2s)$, where s is the dimensionless action[13] $s \sim r_s^{1/2} \ln^{3/2}(l/a)$. Since $s \gg 1$, tunneling paths with returns can be neglected. Therefore, for electron tunneling over distances $x \gg l$ the action s should be multiplied by the number of impurities passed. The average number of such impurities is equal to x/l, which yields the total tunneling probability $P \propto \exp(-2x/\xi_x)$, with ξ_x given by Eq. (5). With a logarithmic accuracy, the effect of the Coulomb gap is to replace g_B by $g(\varepsilon)$ evaluated at the characteristic hopping energy $\varepsilon = \sqrt{T_{ES}^{(0)} T}$, where $T_{ES}^{(0)}$ is defined by Eq. (6). The latter result follows from Eqs. (21) and (5). The final expression for the parameter T_{ES} is given by Eq. (7). We briefly note that in a long enough chain clusters of atypically densely spaced impurities may exist. Tunneling through such segments would cost a higher tunneling action and therefore the overall conductivity would be suppressed. In this paper we assume that the chain is sufficiently short so that these rare clusters can be neglected, see a comment after Eq. (7).

Formulas (6) and (7) indicate that T_{ES} goes down as impurity concentration $N = 1/l$ decreases. This provides a gradual crossover to the metallic behavior in a pure 1D system.

IV. 3D SYSTEM WITH A LARGE IMPURITY CONCENTRATION

In this section we consider a quasi-1D system made of parallel chains which form a periodic array in the transverse directions. The chains are pinned by impurity centers, which divide them into metallic rods of average length $l = 1/Na_\perp^2$, where $a_\perp^2$ is the cross-sectional area per chain. The finite-size electron crystals in each rod are either compressed or stretched to accommodate an integral number of

electrons, as in the case of a single chain. In this section we assume that for a typical rod, the energy of its longitudinal deformation is smaller than the energy of its transverse coupling to rods on the neighboring chains. This can be the case when the periodic potential created by the neighboring chains is diminished because $a_\perp$ is larger than a, and/or when the impurity concentration is large enough. Formally, the inequality $a_\perp \ll l \ll l_s$ needs to be satisfied, where l_s is the soliton length [Eq. (1)]. Since metallic rods now completely fill the 3D space [see Fig. 1(b)], they modify the dielectric constant of the system. As in the interrupted-strand model,[38] the dielectric constant is anisotropic. Along the chain direction it has the value of

$$\kappa_x = \kappa [1 + C_5 (l/r_D)^2], \qquad (22)$$

where $r_D \sim a_\perp$ is the screening length, see Appendix. A, and $C_5 \sim 1$ is a numerical constant.[41] Transverse dielectric constants are unaffected, $\kappa_y = \kappa_z = \kappa$. At large l, κ_x greatly exceeds κ, which leads to an anisotropic Coulomb interaction in the form[42]

$$U(r) = \frac{e^2}{\kappa \sqrt{x^2 + (\kappa_x/\kappa) r_\perp^2}}, \qquad (23)$$

where $r_\perp^2 = y^2 + z^2$. In spite of the large dielectric constant, the Coulomb interaction is long range and thus creates a Coulomb gap. Using the standard ES argument,[4,43] the following density of states of charge excitations is obtained

$$g(\varepsilon) = \frac{3}{\pi} \frac{\kappa^2 \kappa_x}{e^6} \varepsilon^2. \qquad (24)$$

It differs from the conventional formula for an isotropic medium only by the presence of κ_x instead of κ. In order to calculate the VRH conductivity we still have to discuss the tunneling probability. It is important that Eq. (23) holds only at $x \gg l$. The interaction between charge fluctuations on the same rod is short range due to screening by neighboring chains.[44] Tunneling along the x axis takes place similarly to the case of a single chain, but screening of the Coulomb interaction leads to smaller action of the order of $s \sim \sqrt{r_s} \ln(l/a)$. Therefore, for the localization length in the x direction we get

$$\xi_x = \frac{l}{s} \sim \frac{l}{\sqrt{r_s} \ln(l/a)}. \qquad (25)$$

The tunneling in the y and z directions is accomplished by single-electron-like excitations. The probability of tunneling decays exponentially, $P \propto \exp(-2r_\perp/\xi_\perp)$, at large transverse distances $r_\perp$. Here $\xi_\perp$ is the transverse localization length given by Eq. (8) and discussed in more detail in Appendix B. We assume that $\xi_\perp$ is not vanishingly small compared to ξ_x, in which case the VRH has a 3D character and can be calculated by the percolation approach (see Ref. 4, and references therein).[45] This calculation differs from the isotropic case by the replacement of the isotropic dielectric constant κ

and the isotropic localization length ξ by their geometric averages over the three spatial directions:

$$T_{ES} = C_3 \frac{e^2}{(\kappa^2 \kappa_x)^{1/3}} \frac{1}{(\xi_x \xi_\perp^2)^{1/3}}. \tag{26}$$

With the help of Eqs. (22) and (25) the expression for T_{ES} reduces to Eq. (9), where the screening length of the electron crystal has been taken as $r_D \sim a_\perp$ and numerical coefficients absorbed in C_3.

V. 3D SYSTEM WITH A SMALL IMPURITY CONCENTRATION

In this section we study the crystal pinned by impurities with a low concentration N so that the condition $l \gg l_s$ is satisfied. As discussed in Sec. I all key quantities—density of states, localization length, the screening of Coulomb interactions—undergo dramatic changes compared to the case of high impurity concentration. We address such changes in the three separate sections below.

A. Pinning of a quasi-1D crystal by strong dilute impurities

In this section we study the ground-state structure and screening properties of the crystal with low impurity concentration.

We start by reviewing the physical meaning of l_s given by Eq. (1), in which $\alpha = Y_\perp / Y_x$ is the anisotropy parameter, and Y_x, $Y_\perp$ parametrize the energy of an elastic distortion of the crystal,

$$E^{el} = \frac{1}{2} \int d^3r [Y_x (\partial_x u)^2 + Y_\perp (\boldsymbol{\nabla}_\perp u)^2]. \tag{27}$$

As shown in Appendix A, at large r_s the longitudinal elastic modulus Y_x is dominated by Coulomb effects,

$$Y_x \sim e^2 / \kappa a^2 a_\perp^2. \tag{28}$$

The transverse modulus $Y_\perp$ can be substantially smaller than Y_x even when the ratio $a_\perp / a$ is only modestly large. For Coulomb interaction, $Y_\perp \propto \exp(-2\pi a_\perp / a)$.

The energy E^{el} in Eq. (27) is essentially the short-range part of the Coulomb energy. The total energy also includes the long-range Coulomb part (see Appendix A) and the pinning part (see Appendix C and below). Strictly speaking, Eq. (27) is valid only for small gradients of the elastic displacement field $u(\mathbf{r})$; however, it can be used for order-of-magnitude estimates down to microscopic scales $r_\perp \sim a_\perp$ and $x \sim l_s$. In this manner, one can derive formula (1) by minimizing E^{el} under the condition that u changes from 0 to a over a segment of length l_s on a single chain. For more details, see Refs. 27, 23, and Appendix A.

The inequality $l \gg l_s$ imposes the upper limit on the impurity density:

$$N \ll \sqrt{\alpha}/a_\perp^3. \tag{29}$$

Below we show that at such N the ground state of the electron crystal is determined by an interplay of individual and collective pinning.[46]

Without impurities the crystal would have a perfect periodicity and long-range 3D order. Impurities cause elastic distortions of the lattice. The strongest distortions, of dipolar type, are localized in the vicinity of impurities, see Sec. I and Fig. 1(c). Such dipoles have a characteristic size l_s (same as free solitons), are well separated from each other, and occupy only a small fraction of the space. Their creation is advantageous because the associated energy cost (elastic plus Coulomb) is of the order of $W \sim e^2 / \kappa l_s$ per impurity, whereas the energy gain is a much larger electron-impurity interaction energy $-e^2 / \kappa a$. This is the essence of individual (strong) pinning phenomenon, which provides the dominant part of the pinning energy density. The collective (weak) pinning results from interaction between the dipoles. Let us demonstrate that such interaction cannot be neglected at sufficiently large length scales. By solving the elasticity theory equations (generalized to include the Coulomb interactions), it can be shown[27] that a dipolar distortion centered at a point $(x_i, r_{\perp i})$ has long-range tails that decay rather slowly with distance, $u \sim A_i a r_D / \sqrt{\alpha} |x - x_i|$. This displacement is confined mainly within a paraboloid $|r_\perp - r_{\perp i}|^2 \lesssim \sqrt{\alpha} r_D |x - x_i|$. Note that the segment $0 < x < x_{min} \equiv a_\perp (l/\sqrt{\alpha} r_D)^{1/2}$ of the paraboloid,

$$r_\perp^2 = \sqrt{\alpha} r_D |x|, \tag{30}$$

contains on average one impurity. Parameter $r_D \sim a_\perp$, which we already encountered in Sec. IV, has the meaning of the screening length. It is related to the longitudinal elastic modulus Y_x as follows:

$$r_D^2 = \frac{\kappa}{4\pi e^2} a^2 a_\perp^4 Y_x, \tag{31}$$

see Appendix A.

If, in the first approximation, we choose to neglect the interaction among the dipoles, then we should simply add their far elastic fields treating the amplitudes $-1 \lesssim A_i \lesssim 1$ as random variables. We immediately discover the logarithmic growth of u with distance,

$$\langle [\bar{u}(x,0) - \bar{u}(0,0)]^2 \rangle \sim N \int_{x_{min}}^{x} dx' \int_0^{\sqrt{\alpha r_D x'}} dr_\perp^2 \left(\frac{a r_D}{\sqrt{\alpha} x'} \right)^2$$

$$= \left(\frac{a^2}{C_6} \right) \left(\frac{l_s}{l} \right) \ln \left(\frac{x}{x_{min}} \right), \tag{32}$$

where the bar over u indicates that we refer to the value of u away from the immediate vicinity of a dipole and $\langle \cdots \rangle$ stands for disorder averaging.

The logarithmic growth of the elastic displacements was previously derived for the model of *weak* pinning centers in early works[21,22] on the subject. In those calculations the numerical coefficient C_6 is large and is inversely proportional to the impurity strength. In our case $C_6 \sim 1$. Apart from that, Eq. (32) demonstrates that the case of *strong* pinning centers is essentially similar. Therefore, as customary for weak pin-

ning models we define the longitudinal L_x and transverse $L_\perp$ Larkin lengths as the length scales where $\langle \Delta u^2 \rangle \equiv \langle [u(\mathbf{r}) - u(0)]^2 \rangle \sim a^2$. From Eqs. (30) and (32) we obtain

$$L_x = x_{\min} \exp(C_6 l/l_s), \quad L_\perp = r_\perp^{\min} \exp(C_6 l/2l_s), \quad (33)$$

where $r_\perp^{\min} = (\sqrt{\alpha} r_D x_{\min})^{1/2}$.

Alternative derivation of Eqs. (32) and (33) based on energy estimates is given in Appendix C. It elucidates that the slow logarithmic growth of $\langle \Delta u^2 \rangle$ is rooted in the important role of long-range Coulomb interaction in the elastic response of a quasi-1D crystal. An isotropic electronic crystal adjusts to pinning centers primarily by means of shear deformations[47] that do not cost much Coulomb energy. As a result, in the isotropic crystal Δu grows algebraically with distance. In contrast, in quasi-1D crystals and CDW, where the elastic displacement is a scalar (electrons move only along the chains), no separate shear deformations exist. The buildup of the Coulomb energy that accompanies longitudinal compressions translates into an exceptionally large rigidity of the electron lattice and exponentially large L_x and $L_\perp$.

At distances exceeding the Larkin lengths the dipoles can no longer be treated as independent. Indeed, the energy cost E_s of a given dipole is determined by the minimal distance by which the crystal has to distort to align an electron with the impurity position. Therefore, just like the energy of a rod in the previous sections, E_s has a periodic dependence on $\nu = \{(x_i - \bar{u})/a\}$, where $\{\cdots\}$ denotes the fractional part. E_s vanishes at $\nu = 0$ and reaches a maximum value of $\sim W$ at $\nu = \pm 1/2$. Therefore, as soon as the cumulative effect of other dipoles attempts to elevate $|\nu|$ above 1/2, a 2π-phase slip should occur to adjust $E_s(\bar{u})$ to a lower value. The overall effect of such adjustments is to enhance the pinning energy. This additional energy gain can be viewed as the *collective pinning* effect. Using standard arguments (see Appendix C), we relate the extra pinning energy density to the Larkin length

$$\mathcal{E}_{\text{pin}} \sim -W/a_\perp^2 L_x \sim -Y_\perp (a/L_\perp)^2. \quad (34)$$

We will now use this result to estimate the asymptotic value

$$\kappa_x \equiv \epsilon(q_x \to 0, q_\perp = 0) \quad (35)$$

of the longitudinal component of the dielectric function.

Without impurities, the dielectric function has the form

$$\epsilon(\mathbf{q}) = \kappa + \frac{q_x^2}{q^2} \frac{\kappa r_D^{-2}}{q_x^2 + \alpha q_\perp^2}, \quad (36)$$

see Appendix A and, e.g., Ref. 48. Based on previous work[49,22,10] we assume that a reasonable description of dielectric screening in a system with impurities is obtained if we replace the random distribution of pinning centers by a commensurate pinning with the same $\mathcal{E}_{\text{pin}}$. In this case we can use the concept of the dielectric function even for the disordered system. To derive the modified expression for the dielectric function, one can add the term $\mathcal{E}_{\text{pin}}(u/a)^2$ to the right-hand side of Eq. (A2) in Appendix A and repeat the steps outlined thence. It is easy to see that the net effect of

(commensurate) pinning is to augment the combination $q_x^2 + \alpha q_\perp^2$ (proportional to the elastic resorting force) by the term $-\mathcal{E}_{\text{pin}}/Y_\perp a^2$, which comes from the additional restoring force due to impurities. In this manner we obtain

$$\epsilon(\mathbf{q}) = \kappa + \frac{q_x^2}{q^2} \frac{\kappa r_D^{-2}}{q_x^2 + \alpha(q_\perp^2 + L_\perp^{-2})}, \quad (37)$$

$$\kappa_x = \frac{\kappa}{\alpha} \left(\frac{L_\perp}{r_D} \right)^2 = \frac{\kappa}{\sqrt{\alpha}} \frac{L_x}{r_D} \sim \exp\left(C_6 \frac{l}{l_s} \right). \quad (38)$$

However, for our purposes a cruder approximation will be sufficient, namely, we can assume that at distances shorter than the Larkin length, the system screens as though it is free of impurities, Eq. (36); at distances larger than the Larkin length, the dielectric function is replaced by a constant, Eq. (38). In the following section we will use Eqs. (36) and (38) to derive the functional form of the Coulomb gap in the regime $l \gg l_s$.

B. Bare density of states and the Coulomb gap at low impurity concentration

In order to describe the low-T transport at low impurity concentration, $l \gg l_s$, we need to determine the origin of low-energy charge excitations in this regime. This poses a conceptual problem. Indeed, such excitations do not exist in the bulk (away from impurities) where the creation energy of charge-e excitations is bounded from below by the energy W of a 2π soliton. At first glance, the impurities do not help either. As mentioned in Sec. I, near isolated impurities there is an energy gap for charge excitations, which is not much smaller than W. This is because a single impurity appreciably disturbs the crystal only within the region of length l_s. The disturbance is electrically neutral (dipolar) in the ground state. Creation of a charge-e excitation near such an impurity requires an energy of the order of $e^2/\kappa l_s \sim W$. Let us now show that charge excitations of arbitrary low energies nevertheless exist. They come from impurity clusters. Each cluster is a group of a few impurities spaced by distances of the order of l_s or smaller. (It can be viewed as a microscopic inclusion of the $l \lesssim l_s$ phase.) Below we demonstrate that the clusters provide the bare density of states at zero energy, which decreases with l no faster than a power law,

$$g_B = \frac{\kappa}{e^2 a_\perp^2} \left(\frac{l_s}{l} \right)^{\beta+2}, \quad (39)$$

where exponent β is of the order of unity and is independent of l. The calculation of β has to be done numerically, which we leave for future work.

To prove that Eq. (39) gives the lower bound on g_B, consider the configuration of $2M+2$ impurities shown in Fig. 4. The impurities define a cluster of $2M+1$ short rods, each of approximately the same length $c \ll l_s$. The cluster is flanked by two semi-infinite segments at the ends. We assume that M is sufficiently large so that $L = Mc$ is much greater than l_s. Suppose that the length of the central rod in
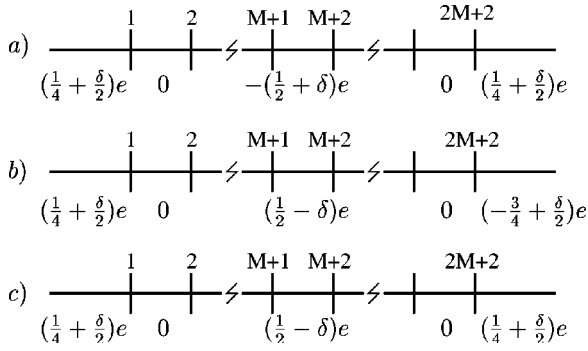
FIG. 4. An example of an impurity cluster that provides low-energy charge excitations at $l \gg l_s$. (a) Distribution of charges in the ground state. For simplicity, we chose $\delta_L = \delta/2$. The cluster is electrically neutral. (b) Competing neutral state. (c) Excited state obtained by increasing the charge of the central rod by one unit.

units of a is close to a half integer, so that the charge of this rod is restricted to the set of values $q = (-1/2 - \delta + n)e$, where n is an integer and $0 < \delta \ll 1$. For the low-energy states we only need to consider two possibilities, $q = (-1/2 - \delta)e$ and $(1/2 - \delta)e$. The lengths of the other short rods in our construction are chosen to be close to integer multiples of a. Then those rods can be considered charge neutral. Finally, we assume that the position of the leftmost impurity restricts the charge of the left semi-infinite cluster to $1/4 + \delta_L + n_L$, where $|\delta_L| \ll 1$ and n_L is another integer. Under these assumptions, the charge of the right semi-infinite segment is fixed to the set $1/4 + \delta - \delta_L + n_R$.

One possible candidate for the ground state is the charge configuration shown in Fig. 4(a). It is overall neutral, has the charge of the central rod equal to $q = (-1/2 - \delta)e$, and the total energy

$$E_a = \frac{2}{L\kappa} \frac{e}{4} \left(-\frac{e}{2} \right) + \frac{1}{2L\kappa} \left(\frac{e}{4} \right)^2 + \frac{e^2 (1/2 + \delta)^2}{2C_r} + 2W_{1/4}$$

$$= -\frac{7}{32} \frac{e^2}{L\kappa} + \frac{e^2}{2C_r} (1/2 + \delta)^2 + 2W_{1/4}. \tag{40}$$

Here we made use of the conditions $L \gg l_s$, $\delta \ll 1$. $W_{1/4}$ denotes the self-energies of the semi-infinite segments (which contain "1/4 solitons"), and $C_r \sim \kappa c$ is the self-capacitance of the central rod. If the configuration shown in Fig. 4(a) is indeed a ground state, it has an unusual feature that the charge of the central rod exceeds 1/2 by the absolute value, contrary to the arguments in Sec. III. To establish the conditions for the cluster to have such a ground state, we need to compare E_a with energies of other possible states. Of those, some are neutral and some are charged. One competing neutral state is shown in Fig. 4(b). It has energy

$$E_b = -\frac{11}{32} \frac{e^2}{L\kappa} + \frac{e^2}{2C_r} (1/2 - \delta)^2 + W_{1/4} + W_{3/4}, \tag{41}$$

where $W_{3/4}$ is the energy of the "3/4 soliton" on the right of the cluster in Fig. 4(b). For the energy difference we have

$$E_b - E_a = \frac{e^2}{C_r} \delta - \frac{1}{8} \frac{e^2}{L\kappa} + W_{3/4} - W_{1/4}, \tag{42}$$

so that the state shown in Fig. 4(a) wins if

$$\delta < \frac{C_r}{e^2} \left[(W_{3/4} - W_{1/4}) - \frac{1}{8} \frac{e^2}{L\kappa} \right]. \tag{43}$$

Since $W_{3/4} - W_{1/4} \sim W \sim e^2 / \kappa l_s$ and $L \gg l_s$, the right-hand side of the inequality (43) is positive, and so $\delta > 0$ that satisfy such an inequality do exist. The only other viable competing neutral state is similar to that shown in Fig. 4(b) except the 3/4 soliton is formed on the left semi-infinite segment. The energy of that state is also E_b, and so it does not lead to any further restrictions on δ.

Now let us examine the charged states. There is only one viable competitor, with $q = (1/2 - \delta)e$, as shown in Fig. 4(c). If the energy difference $\varepsilon = E_c - E_a$ is positive, then Fig. 4(a) represents the true ground state and ε gives the creation energy of the charge-e excitation. If ε is negative, then the ground state is as shown in Fig. 4(c), while the charge and the energy of the lowest-energy charge excitation are equal to $-e$ and $-\varepsilon$, respectively. An elementary calculation yields

$$\varepsilon = -\frac{e^2}{C_r} \delta + \frac{e^2}{2\kappa L}, \tag{44}$$

from which we conclude that it is possible to obtain arbitrary small ε of both signs by tuning δ sufficiently close to $C_r / 2L\kappa \sim c/L$, without violating the inequality (43). This proves that clusters are able to produce a finite $g_B(0)$. In the ground state some of these clusters are neutral ("empty") and some are charged ("occupied").

Now let us try to estimate g_B due to clusters. In the above argument we required strong inequalities $c \ll l_s$ and $L \gg l_s$ to prove the existence of a nonzero g_B with mathematical rigor. Physically, it seems reasonable that such inequalities can be softened to $c \lesssim l_s$ and $L \gtrsim l_s$, in which case $\delta \lesssim 1$ and $M \sim 1$, i.e., only a few (of the order of unity) impurities are needed. It is also clear that the rods to the left and to the right of the central one need not be exactly neutral for the argument to go through. Then the probability of forming the desired cluster is comparable to the probability of finding $2M + 2$ (a few) impurities on the same chain with nearest-neighbor separation less than l_s. Assuming that impurity positions are totally random and independent, we obtain the estimate of Eq. (39).

Now let us calculate the form of the Coulomb gap in the actual density of states $g(\varepsilon)$. At exponentially small energies, $\varepsilon \ll \varepsilon_* = e^2 / \kappa L_x$, the Coulomb gap is determined by the interactions on distances exceeding the size of the Larkin domain. At such distances the interaction has the form (23), leading to the usual parabolic Coulomb gap given by Eqs. (24) and (38). We put these equations side by side below for the ease of reading,

$$g(\varepsilon) = \frac{3}{\pi} \frac{\kappa^2 \kappa_x}{e^6} \varepsilon^2, \quad \varepsilon \ll \varepsilon_*, \tag{45}$$

$$\varepsilon_* = \frac{e^2}{\kappa L_x} = \frac{e^2}{\sqrt{\alpha} r_D} \frac{1}{\kappa_x}, \tag{46}$$

$$\kappa_x \sim \exp\left(C_6 \frac{l}{l_s} \right). \tag{47}$$

To ascertain the region of validity of Eq. (45) one needs to make sure that $g(\varepsilon)$ does not exceed the bare density of states g_B. It is easy to see that this is the case here. At the largest energy $\varepsilon \sim \varepsilon_*$ [Eq. (46)], $g(\varepsilon)$ is exponentially small, $g \propto \exp(-C_6 l/l_s)$, and so it is indeed much smaller than $g_B \sim (l_s/l)^{\beta+2}$. In this sense g_B is large enough to ensure the validity of the parabolic law over the full range of ε specified in Eq. (45).

At ε larger than ε_*, the Coulomb gap is governed by interactions within the volume of a Larkin domain and the dispersion of the dielectric function $\epsilon(\mathbf{q})$ becomes important. The interaction potential is defined by $\tilde{U}(\mathbf{q}) = 4\pi e^2/\epsilon(\mathbf{q})q^2$ and Eq. (37) in the q space. In real space, it is given by[27]

$$U(\mathbf{r}) \simeq \frac{e^2}{2\kappa |x|} \exp\left(-\frac{1}{4\sqrt{\alpha}} \frac{r_\perp^2}{r_D|x|} \right), \tag{48}$$

$$a_\perp \ll r_\perp \ll \min\{\sqrt{\alpha}|x|, L_\perp\}, \quad \frac{r_D}{\sqrt{\alpha}} \ll x \ll L_x. \tag{49}$$

The potential $U(\mathbf{r})$ is appreciable only within the paraboloid defined by Eq. (30), where it behaves as $U(r) \simeq e^2/2\kappa|x|$. A more precise statement is that the surface of a constant U is a paraboloidlike region

$$r_\perp^2 \simeq 4\sqrt{\alpha} r_D |x| \ln\left(\frac{e^2}{2U\kappa|x|} \right). \tag{50}$$

For $U \gg \varepsilon_*$, this surface belongs to the domain (49) where Eq. (48) holds.

To calculate the functional form of the Coulomb gap we use the self-consistent mean-field approximation due to Efros,[43] according to which g is the solution of the integral equation

$$g(\varepsilon) = g_B \exp\left[-\frac{1}{2} \int_0^W d\varepsilon' g(\varepsilon') V(\varepsilon+\varepsilon') \right], \tag{51}$$

where $V(U)$ is the volume enclosed by the constant-U surface (50),

$$V(U) \simeq \frac{\pi\sqrt{\alpha}}{4} \frac{e^4 r_D}{\kappa^2 U^2}. \tag{52}$$

Equation (51) follows from the requirement that the ground state must be stable agaisnt a transfer of a unit charge from an occupied state with energy $-\varepsilon'$ to an empty state with energy ε. Such a stability criterion[28,4] can be expressed by means of the inequality $\varepsilon + \varepsilon' - U(\mathbf{r}) > 0$, where $\mathbf{r}$ is the vector that connects the two sites. Thus, the integral on the right-hand side of Eq. (51) counts the pairs of states that would violate the stability criterion if positioned randomly.
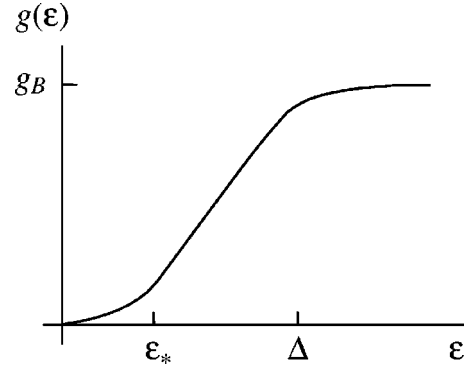

FIG. 5. The density of states of charge excitations in a 3D system with $l \gg l_s$. The parabolic Coulomb gap at low energies is succeeded by the linear Coulomb gap, then by the bare density of states g_B created by impurity clusters.

The Coulomb gap can be viewed as the reduced statistical weight of stable ground-state charge distributions with respect to that of the totally uncorrelated ones.

The solution of Eq. (51) has the asymptotic form

$$g(\varepsilon) \simeq \frac{8}{\pi\sqrt{\alpha}} \frac{\kappa^2}{r_D e^4} |\varepsilon|, \quad \varepsilon_* \ll |\varepsilon| \ll \Delta. \tag{53}$$

We see that the unusual interaction potential of Eq. (48) leads to a nonstandard Coulomb gap, which is linear in a 3D system. The weaker (linear instead of the standard quadratic) suppression of g is due to a metallic screening of the Coulomb potential in the major fraction of solid angle. The energy scale Δ in Eq. (53) is defined by the relation $g(\Delta) \sim g_B$. Using Eq. (39), we can estimate Δ as follows:

$$\Delta = \frac{\sqrt{\alpha} r_D}{\kappa^2} e^4 g_B \sim W\left(\frac{l_s}{l} \right)^{\beta+2}. \tag{54}$$

At $\varepsilon \gg \Delta$, the solution of Eq. (51) approaches the bare density of states, $g \simeq g_B$, and so Δ has the meaning of the Coulomb gap width. On the lower-energy side, at $\varepsilon \sim \varepsilon_*$, the linear Coulomb dependence of Eq. (53) smoothly matches the quadratic dependence of Eq. (45). All such dependencies are summarized in Fig. 5.

C. VRH transport in a system with small impurity concentration

The VRH transport at $l \gg l_s$ involves quantum tunneling of charge excitations between rare impurity clusters. In Appendix B we advance arguments that the charge tunnels along the chains in the form of 2π solitons and derive the following estimate for the corresponding longitudinal localization length:

$$\xi_x \sim \frac{l_s}{\sqrt{r_s}} \left[1 + \frac{l_s}{l} \ln\left(\frac{l_s}{a} \right) \right]^{-1}, \quad l > l_s. \tag{55}$$

At $l \gg l_s$ this formula goes over to Eq. (12), while at $l \sim l_s$ it smoothly matches with Eq. (25). As for the interchain tunneling, it is still accomplished by single-electron-like excita-

tions and the corresponding localization length $\xi_\perp$ is still given by Eq. (8), see Appendix B. We will assume that $\xi_\perp/a_\perp$ is not vanishingly small, in which case the VRH has the 3D character.[45]

The density of states and localization lengths is all the information we need to calculate the VRH conductivity. A more complicated dependence of the density of states $g(\varepsilon)$ on energy in the case at hand, $l > l_s$, brings about a larger variety of possible transport regimes.

At the lowest temperatures we still have the ES law with parameter T_{ES} given by Eq. (26). Due to the exponential growth of the longitudinal dielectric constant κ_x with l [Eq. (38)], T_{ES} decreases exponentially, $T_{ES} \propto \exp(-C_6 l/3 l_s)$. This dependence entails a precipitous drop of $-\ln \sigma$ as a function of l, as soon as l exceeds l_s, see Fig. 2. Such an enhancement of the conductivity is due to progressively more efficient screening of the long-range Coulomb interactions (steeply increasing κ_x), which enhances the density of states inside the Coulomb gap, see Eq. (45).

The ES law (2) holds until the range of ε's that contribute to the VRH transport,[4] $|\varepsilon| \lesssim (T T_{ES})^{1/2}$, fits inside the parabolic part of the Coulomb gap, $|\varepsilon| \lesssim \varepsilon_*$. For a fixed $T \ll W$ this gives the condition $l \lesssim l_s \ln(W/T)$.

At larger l, the unusual linear Coulomb gap (53) leads to the 2/5 law for the VRH transport [Eq. (13)], which we reproduce below for convenience,

$$\sigma = \sigma_0 \exp[-(T_1/T)^{2/5}]. \tag{56}$$

As emphasized in Sec. II, parameter T_1 is impurity independent and is, in this sense, universal, see Eq. (14). This behavior leads to the intermediate plateau at the graph in Fig. 2.

The range of energies that contributes to the VRH in the 2/5-law regime is given by $|\varepsilon| \lesssim (T_1/T)^{2/5} T$. At $l \sim l_s (W/T)^\gamma$, where $\gamma = 3/[5(\beta+2)] \lesssim 0.3$, this range becomes broader than the Coulomb gap width Δ [Eq. (54)]. At such and larger l, the Coulomb gap can be neglected, and the VRH begins to follow the usual Mott law [Eq. (15)]

$$\sigma = \sigma_0 \exp[-(T_M/T)^{1/4}], \tag{57}$$

with parameter T_M increasing with l according to $T_M \propto 1/g_B \propto (l/l_s)^{\beta+2}$. The growing T_M leads to exponentially increasing resistivity, represented by the ascending branch of the curve in Fig. 2. Physically, the suppression of the dc conductivity stems from decreasing density of low-energy states available for transport, just like in conventional doped semiconductors[3,4] or commensurate CDW systems.[39]

VI. CONCLUSIONS AND COMPARISON WITH EXPERIMENT

It is widely recognized that interactions must play a significant role in determining the properties of 1D and quasi-1D conductors, because in such materials the dimensionless strength of the Coulomb interaction is very large, $r_s \gg 1$. In the presence of impurities, these systems behave as insulators and do not possess metallic screening. Thus, the interactions are both strong and long range. Our main goal in this paper was to understand the effect of such interactions
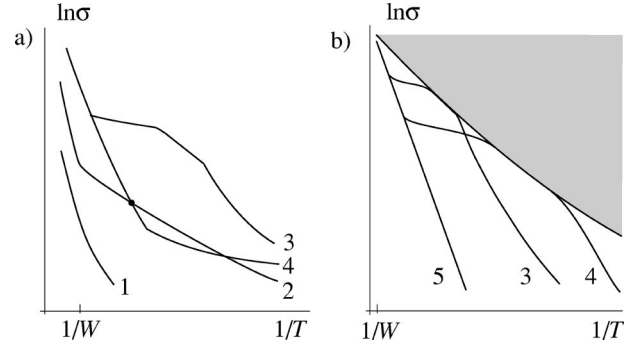

FIG. 6. Logarithm of the conductivity vs the inverse temperature for several samples labeled in the order of increasing l, i.e., sample purity. (a) Curve 1 corresponds to $l = l_1 < l_s$ and displays only the ES regime. The higher-T activation regime is beyond the limits of the graph. Curve 2 is for $l = l_2 \gtrsim l_s$, and so the both the activation behavior and the ES law are visible. Curve 3 is for $l = l_3 \gtrsim l_2$. It shows the complete sequence of the transport regimes: the activation, Mott, 2/5, and ES laws. Curve 4 depicts the behavior of a sample with an impurity concentration another notch lower than that of sample 3. In panel (a) it goes through the activation and the Mott regimes. In panel (b) that covers considerably lower T, curve 4 also exhibits the 2/5 law, followed by the ES law. The 2/5 law is shown by the solid line along the lower edge of the shaded region. The curves can skim along this line but cannot cross it. The higher the sample purity the lower the temperature at which the sample starts to exhibit the 2/5 law but also the wider the range of T over which this law persists. Curve 5 depicts the case $l \gg l_s$ where any kind of VRH transport corresponds to Ohmic resistances higher than the experimental measurement limit, so that only the activated transport can be observed.

on the nature of the low-energy charge excitations and their Ohmic dc transport. To that end we formulated a generic model of an anisotropic electron system with strong Coulomb interactions and disorder and presented its theoretical analysis. We elucidated the origin of the low-energy charge excitations in this model and demonstrated that their density of states possesses a soft Coulomb gap. In 3D case, we found that the Coulomb gap exhibits a power-law dependence on the energy distance from the Fermi level. We discussed how the prefactor and the exponents of this power law vary as a function of the impurity concentration and other parameters of the model. We also discussed how the Coulomb gap is manifested in the variable-range hopping conductivity at low temperatures.

One of the central results of our theory is a nonmonotonic dependence of σ on the impurity concentration N, as shown in Fig. 2, where we sketched σ as a function of $l = 1/N a_\perp^2$, i.e., as N decreases, at fixed T. As clear from that figure and the discussion in Sec. II, at large N the conductivity increases as N decreases, similar to behavior found in metals. In contrast, at small N the conductivity drops as N goes down, which resembles the behavior of doped semiconductors. For intermediate N, our theory predicts the existence of an N-independent plateau.

Another way to represent these theoretical predictions, common in semiconductor physics, is shown in Fig. 6. In that figure the dependence of the logarithm of conductivity

on the inverse temperature is depicted for a series of samples, each with fixed N. An unusual circumstance illustrated by Fig. 6 is the crossing of the curves that correspond to different samples. In Fig. 6(a) we show that up to two crossing points may exist between one curve that corresponds to $l<l_s$ (curve 2) and another curve for $l>l_s$ (curve 4). The higher-T crossing occurs when the curve 4 goes through the activation regime, the lower-T one—when it exhibits the Mott VRH. The dirtier ($l<l_s$) sample obeys the ES behavior in both instances. Another property we tried to emphasize in Fig. 6 is the role of the 2/5 law as the upper bound of the conductivity regardless of the sample purity. For samples with low impurity concentration the 2/5 law is also the envelope curve, see Fig. 6(b).

Let us now turn to the experimental situation. The transport behavior of a number of organic compounds, including TMTSF-DMTCNQ, TTF-TCNQ, and NMe-4-MePy (TCNQ)$_2$, is indeed in a qualitative agreement with our theory. It should be clarified that such materials form CDW phases that in addition to the usual $2k_F$ periodicity, have an appreciable or, in some cases, even predominant $4k_F$ harmonics. The latter is considered the evidence for the strong Coulomb interaction,[11] and so is precisely the case we studied in this paper.

In the experiments of Zuppiroli et al.[50,35] the transport in the aforementioned compounds was studied as a function of defect concentration, which was varied in situ by irradiation of samples by high-energy particles. Admittedly, the nature of the such defects is not known with certainty. Some suggestions in the literature include atomic displacements, broken bonds, polymer cross linking, and charged radicals. At the same time, the effect of the irradiation on transport seem not to depend much on the type of particles used (x rays, neutrons, or electrons) and instead to correlate primarily with the total absorbed energy.[35] This fact is interpreted as evidence that microscopically different defects influence the transport in electron crystals in a similar way, so long as they act as strong localized pinning centers. Under this assumption, it is legitimate to compare the data from the irradiation experiments with our theory even though so far we assumed that defects are created by charged acceptors (see Sec. I). We do so in some detail below.

In Fig. 7 we show an extensive set of data on transport in irradiated TMTSF-DMTCNQ that we assembled by digitizing Fig. 2 of a review paper by Zuppiroli,[35] and original references therein. Apparently, some data series in this figure represent the same sample with successively increasing radiation dose, and some correspond to physically different specimens. For simplicity, we refer to all of them as different samples. The percentage labels on the plot are the estimates of the molar concentrations of defects c quoted by the experimentalists. The points on the $c=0$ trace are from an unirradiated sample.

As shown in Fig. 7, the data for the two most disordered samples can be successfully fitted to the activation law and the next two samples—to the ES formula. This transition from the activation to the ES law with increasing disorder is in agreement with our theory (cf. curves 1 and 2 in Fig. 6). The obtained fit parameters E_A and T_{ES} are given in Table II.
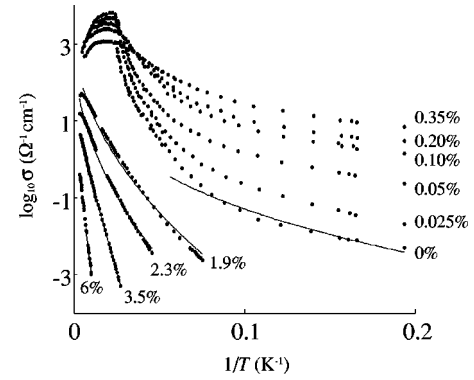

FIG. 7. Low-temperature conductivity of TMTSF-DMTCNQ samples damaged by x-ray radiation. The dots on $c\geq1.9\%$ and $c\leq0.35\%$ curves were generated by digitizing the experimental data in Fig. 1 of Ref. 51 and Fig. 2 of Ref. 35, respectively. The percentages stand for the defect concentrations quoted in those papers. The solid line through the 6% and 3.5% data are the best fits to the activation; through 2.3% and 1.9%—to the ES law. In both cases the prefactors (σ_A and σ_0) were taken to be T independent. The thin line through the 0% data (unirradiated sample) is the best fit to the Mott law based on the $T<20$ K points.

Both E_A and T_{ES} scale roughly linearly c, in agreement with Eqs. (11) and (9). From Eq. (10) we deduce that $\kappa lc=\kappa a \sim 1$ nm, which has the correct order of magnitude (assuming $\kappa\sim1$). One should keep in mind here that the absolute numbers for c were obtained by the authors of Ref. 51 using certain arguable assumptions. In our opinion, the scaling with c may be more reliable than the absolute values quoted because (if no annealing occurs) the relative magnitude of c should scale linearly with the irradiation time, known to experimentalists without any fitting parameters. Combining Eqs. (9) and (11) we further deduce that $a_\perp/\xi_\perp$ and l/ξ_x ratios are some modest numbers less than ten, as may be expected from Eqs. (25) and (8).

As a final remark on high-disorder samples, we would like to mention that the scaling of the longitudinal dielectric constant κ_x with the defect concentration (irradiation time) consistent with Eq. (22) was reported in a separate set of experiments on Qn(TCNQ) by Janossy et al.[52] Together with the transport data, this makes a compelling case for the validity of the metallic-rod (interrupted-strand) model for organic electron crystals with $l\ll l_s$. For such systems we can claim a semiquantitative agreement with the experiment.

Let us now turn to the conductivity of weakly damaged samples.[35] As one can see from Fig. 7 they show metallic behavior at high T, a conductivity maximum at the Peierls temperature of about 42 K, and a decrease in σ, i.e., the

TABLE II. Fitting parameters for data displayed in Fig. 7.

Quoted defect concentration c (%)	T_{ES} (K)	E_A (K)
~6		900
3.5		380
2.3	2800	
1.9	3700	

semiconducting behavior, at lower T. As T drops by a factor of 2 or so below the Peierls temperature, the decrease of σ with $1/T$ becomes considerably more gentle than an activation law. One cannot help noticing a similarity between the behavior of $c = 1.9\%, 0.35\%$, and 0% samples in Fig. 7 and curves 1, 3, and 4, respectively, in Fig. 6. There is also an unambiguous evidence for the existence of the crossing point between, e.g., $c = 0\%$ and $c \approx 1.2\%$ traces at $T = 21$ K (see below). However, an attempt to fit the $c = 0\%$ data to the Mott law is not particularly successful, see Fig. 7. Therefore, we only wish to emphasize a qualitative agreement with our prediction that for a fixed T, the conductivity of "clean" and "dirty" samples should show opposite trends, see Figs. 2 and 6. Indeed, the conductivity of the low-disorder samples ($c \leq 0.35\%$) increases with the radiation dose in contrast to the behavior shown by the high-disorder samples ($c \geq 1.9\%$) where it decreases. In fact, another experiment showed this contrasting behavior in a great detail. In that experiment,[51] $\ln \sigma$ was measured at the fixed temperature of $T = 21$ K, while defect concentration was varied essentially continuously over the range of $0\% < c < 2.5\%$. It was found that σ initially increases by two orders of magnitude, reaches a maximum, and then drops by five orders of magnitude as a function of c. Overall, this is in a qualitative agreement with Fig. 2 except instead of the well-defined 2/5 plateau, $\ln \sigma$ shows only a broad maximum. Similar features are demonstrated also by TTF-TCNQ and NMe-4-MePy (TCNQ)$_2$, see Fig. 1 in Ref. 50, and Figs. 11 and 12 in Ref. 35. We conclude that for low-disorder CDW organics our theory agrees with experiment in some gross qualitative features. The quantitative agreement cannot be verified because the dynamical range of measured conductivities is too narrow. Further low-temperature experiments are desired to clarify the situation and to prove or disprove the existence of the 2/5 law.

Let us now switch to inorganic CDW. Several comments are in order. The electron-electron interactions in these materials are also very strong,[10,53] $r_s \sim 100$. However, inorganic CDW are predominantly $2k_F$, and there is an ample evidence for the important role of the electron-phonon coupling in the CDW dynamics. This coupling can lead to an enhancement of the electron effective mass[49,10] that would result in a short localization length. If the mass enhancement is indeed large, the VRH transport should be observable only in materials with short hopping distances, i.e., large impurity concentrations. Examples include highly doped bronzes[34] and perhaps, the Pt-chain compound KCP.[54,55] From this perspective, the reports of a VRH-like transport in a relatively pure samples of TaS$_3$ [Refs. 56 and 57] and blue bronze [Refs. 58 and 59] are puzzling and require further investigations.

Finally, let us comment on another broad class of quasi-1D systems, conducting polymers. In comparison to CDW, polymers have a much higher degree of structural disorder and a complex morphology that depends on the preparation method. Typical samples contain a mixture of crystalline and amorphous regions, with the correlation length[60] of the order of 10 nm. In the undoped state polymers are commensurate CDW semiconductors with a Peierls-Mott energy gap[2] ~ 1 eV. Doping shifts these systems away from com-

mensurability point and suppresses the gap but it is often inhomogeneous and is an additional source of disorder. At low and moderate doping the T dependence of the conductivity often resembles ES and/or Mott VRH laws, see a short review in Ref. 37. A systematic study of the VRH conductivity dependence on doping has been attempted by Aleshin *et al.*[61] In those experiments doping of poly(3,4-ethilenedioxythiophene/poly(sterenesulfonate) (PEDT/PSS) samples was varied by controlling the pH of the solution at the sample preparation stage. It was observed that at pH < 4 the VRH exponent λ [Eq. (17)] was close to 0.5 and T_{VRH} decreased with pH, while at larger pH, λ was close to $0.4 = 2/5$ and T_{VRH} did not depend on pH. This resembles the behavior that follows from our theory, provided the concentration of the pinning centers decreases with pH. We leave the tasks of extending our theory to the case of conducting polymers and explaining these intriguing experimental results for future investigations.

APPENDIX A: DIELECTRIC FUNCTION AND ELASTICITY IN A CLEAN QUASI-1D ELECTRON CRYSTAL

In this section we derive expressions for the elastic moduli and the dielectric function of a pure crystal.

Following the literature on interacting 1D electron systems[16] and CDW,[49] we describe dynamics of electrons on ith chain by a bosonic phase field $\varphi_i(x,t)$. The long-wavelength components of electron density n_i is related to φ_i by $n_i = \partial_x \varphi_i / 2\pi$. The elasticity theory of the system can be formulated by identifying the elastic displacement u with $(2\pi/a)\varphi$ and taking the continuum limit. Neglecting weak interchain tunneling and dynamical effects we choose our starting effective Hamiltonian H in the form

$$H = \int dx [H_0 + H_C], \tag{A1}$$

$$H_0 = \frac{1}{2} C_x^0 \sum_i n_i^2 + \sum_{ij} J_{ij} \cos(\varphi_i - \varphi_j), \tag{A2}$$

$$H_C = \frac{1}{2} \sum_{ij} \int dx dx' n_i(x) U_{ij}(x - x') n_j(x'). \tag{A3}$$

Let us briefly describe the notations here. The Hamiltonian is split into the short-range (H_0) and the long-range Coulomb (H_C) parts. J_{ij} represents the Coulomb coupling between the CDW modulations of electron density on chains i and j. C_x^0 is the charge compressibility of a single isolated chain. In a

large-r_s 1D system C_x^0 is dominated by the exchange-correlation effects, leading to[62]

$$C_x^0 \sim -\frac{2e^2}{\kappa}\ln\frac{a}{R}, \tag{A4}$$

where R is the characteristic radius of the electron charge form factor in the transverse direction, i.e., the "radius" of the chain. In most physical realizations, we expect $R \ll a$ and *negative* C_x^0. The positivity of the elastic modulus of the system, required for thermodynamic stability, is recovered once we take into account the long-range part H_C of the interaction energy, parametrized by the kernels U_{ij}. U_{ij} is defined as the bare Coulomb kernel $U_0(r)=e^2/\kappa r$ convoluted with the single-chain form factors F, e.g., $F(\mathbf{q}_\perp) = \exp(-q_\perp^2 R^2)$.

We are interested in a linear response where the cosines in Eq. (A2) can be expanded in φ thereupon the effective Hamiltonian becomes quadratic. If an external electrostatic potential $\tilde{V}_{\text{ext}}(\mathbf{q})$ acts on the system, the total equilibrium potential $\tilde{V}(\mathbf{q})$ will in general contain Fourier harmonics with wave vectors $\mathbf{q}+\mathbf{G}$, where $\mathbf{G}$ are the reciprocal vectors of the 2D lattice formed by the transverse coordinates of the centers of the chains. We define the dielectric function $\epsilon(\mathbf{q})$ of the system as the ratio $\tilde{V}_{\text{ext}}(\mathbf{q})/\tilde{V}(\mathbf{q})$ for $\mathbf{q}$ in the Brillouin zone of this lattice. Via standard algebraic manipulations in the reciprocal space we arrive at

$$\epsilon(\mathbf{q}) = \kappa + \frac{4\pi e^2}{a_\perp^2}\frac{q_x^2}{q^2}\frac{1}{B_x(\mathbf{q})q_x^2 + B_\perp q_\perp^2}, \tag{A5}$$

$$B_x(\mathbf{q}) = C_x^0 + \frac{4\pi e^2}{\kappa a_\perp^2}\sum_{\mathbf{G}\neq 0}\frac{F^2(\mathbf{G})}{q_x^2+(\mathbf{q}_\perp+\mathbf{G})^2}, \tag{A6}$$

$$B_\perp = 4\pi^2 a_\perp^2\sum_j J_{ij}. \tag{A7}$$

In the limit $q_x \ll a^{-1}$, $q_\perp \ll a_\perp^{-1}$ we obtain Eq. (36) reproduced below for convenience,

$$\epsilon(\mathbf{q}) = \kappa + \frac{q_x^2}{q^2}\frac{\kappa r_D^{-2}}{q_x^2 + \alpha q_\perp^2}. \tag{A8}$$

Here $r_D = (C_x\kappa/4\pi e^2)^{1/2}a_\perp$ is the Thomas-Fermi screening radius, $C_x > 0$ is the effective charge compressibility of the system,

$$C_x = C_x^0 + \frac{4\pi e^2}{\kappa a_\perp^2}\sum_{\mathbf{G}\neq 0}\frac{F^2(\mathbf{G})}{G^2} \sim \frac{2e^2}{\kappa}\ln\frac{a_\perp}{a}, \tag{A9}$$

and $\alpha = B_\perp/C_x$ is the dimensionless anisotropy parameter. Let us now discuss some consequences of Eq. (A8).

(i) The dielectric function has the same form as in quasi-1D systems with small r_s (see, e.g., Ref. 48).

(ii) The screening radius r_D is of the order of the interchain separation $a_\perp$. Therefore, Brazovskii and Matveeen-

ko's results[27] for the soliton energy W and the soliton length l_s remain qualitatively correct[63] for high r_s provided we use $r_D \sim a_\perp$.

(iii) The interaction energy $U(\mathbf{r})$ of two pointlike test charges separated by a large distance $\mathbf{r}$ can be calculated by the Fourier inversion of

$$\tilde{U}(\mathbf{q}) = \frac{4\pi e^2}{\epsilon(\mathbf{q})q^2}. \tag{A10}$$

For $\alpha x^2 + r_\perp^2 \gg r_D^2$ one finds (cf. Ref. 27)

$$U(\mathbf{r}) \simeq \frac{e^2}{2\kappa|x|}\exp\left(-\frac{1}{2r_D}\frac{r_\perp^2}{\sqrt{\alpha x^2 + r_\perp^2} + \sqrt{\alpha}|x|}\right). \tag{A11}$$

The potential $U(\mathbf{r})$ is not exponentially small only within the paraboloid $r_\perp^2 \lesssim \sqrt{\alpha}r_D|x|$ [cf. Eq. (30)]. At the surface of such a paraboloid we have $r_\perp \ll \sqrt{\alpha}|x|$ and $U(\mathbf{r})$ acquires a simpler form quoted in Sec. V,

$$U(\mathbf{r}) \simeq \frac{e^2}{2\kappa|x|}\exp\left(-\frac{1}{4\sqrt{\alpha}}\frac{r_\perp^2}{r_D|x|}\right). \tag{A12}$$

(iv) Finally, the effective longitudinal and transverse elastic moduli of the system are given by

$$Y_x = \frac{C_x}{a^2 a_\perp^2} \sim \frac{e^2}{\kappa a^2 a_\perp^2}, \tag{A13}$$

$$Y_\perp = \alpha Y_x. \tag{A14}$$

APPENDIX B: TUNNELING IN A 3D CRYSTAL WITH A LOW IMPURITY CONCENTRATION

The localization lengths $\xi_\perp$ and ξ_x needed for calculation of the VRH transport are determined by long-distance tunneling of charge excitations. The problem of tunneling is nontrivial because a broad spectrum of charge excitations exists. Leaving more detailed investigations for future work, we concentrate on two possible tunneling mechanisms: by electronlike quasiparticles and by many-body excitations, the 2π solitons.

In the quasiparticle mechanism the charge is carried by a single electron while all other electrons remain unperturbed in their quantum ground states. The rational for examining this mechanism is its minimal possible tunneling mass. The problem of calculating ξ_x and $\xi_\perp$ reduces to the quantum mechanics of a single particle in a fixed external potential. Clearly, the optimal tunneling path should go through the interstitial positions where the energy barrier is the lowest. It is convenient then to formulate the problem as a problem on a lattice of such interstitial positions. The relevant variables are the on-site energies and the hopping matrix elements. The on-site energies are all equal to $\varepsilon_{\text{int}} \sim e^2/\kappa a$. The hopping terms for the interchain tunneling, $t_\perp$, are determined by the band structure in the case of tunneling inside a chemically synthesized materials. In the case of tunneling between

distant 1D conductors $t_\perp \propto \exp(-a_\perp/a_B)$. The hopping matrix element for tunneling along the chain, t_x, can be estimated straightforwardly, with the result $t_x = \varepsilon_{int} \exp(-C_7 \sqrt{r_s})$, $C_7 \sim 1$. In the absence of impurities, the problem is reduced to the propagation through a periodic lattice. The eigenstates in that model are labeled by wave vectors $\mathbf{k}$, according to the tight-binding dispersion relation

$$\varepsilon_{tb}(\mathbf{k}) = \varepsilon_{int} - 2t_x \cos(k_x a_\perp) - 2t_\perp [\cos(k_y a_\perp) + \cos(k_z a_\perp)].$$

Below the band edge $\varepsilon = \varepsilon_{int} - 2t_x - 4t_\perp$, the eigenstates are exponentially decaying with distance. The corresponding localization (decay) lengths can be related to the imaginary parts of the complex $\mathbf{k}$ solution of the equation $\varepsilon_{tb}(\mathbf{k}) = \varepsilon$. In the case of interest, $\varepsilon \ll \varepsilon_{int}$; $t_\perp, t_x \ll \varepsilon_{int}$, we obtain

$$\xi_x^q = \frac{a}{\ln(\varepsilon_{int}/2t_x)} \sim \frac{a}{\sqrt{r_s}}, \tag{B1}$$

$$\xi_\perp^q = \frac{a_\perp}{\ln(\varepsilon_{int}/2t_\perp)}, \tag{B2}$$

where the superscript q stands for "quasiparticle." Although Eq. (B2) was derived for a clean system, it is clear that impurity do not affect this result unless present in gigantic concentrations ($l \sim a$). Indeed, an individual impurity can modify the local on-site energy by at most a numerical factor, while $\xi_{\perp(x)}$ depend on the on-site energy only weakly, logarithmically. In principle, impurity clusters with atypically low on-site energies, resonant with ε, do exist but as well known from the analysis of the resonant tunneling problem in random systems, such events are exponentially rare and do not contribute to the bulk localization length in any appreciable manner.

Let us now turn to the soliton mechanism, we attempt to profit from the fact that in the bulk, the soliton is the charge excitation of the lowest possible energy, so that the energy barrier could perhaps be lower and the tunneling more effective. However, in the case of interchain tunneling, this is not the case. Indeed, the direct tunneling of a soliton to a different chain is impossible because the soliton is a composite many-body excitation. The closest to the interchain soliton tunneling that one can imagine is a two-stage process, where, one electron first tunnels to the adjacent chain, and then, on the second stage, it pushes away other electrons in the region of length l_s to form a soliton. Since the initial energy barrier is still ε_{int} and the charge spreading only increases the tunneling action, it is clear that such a contrived process offers no advantage compared to the simple one-stage quasiparticle mechanism. Therefore, $\xi_\perp$ is determined by the latter and coincides with $\xi_\perp^q$, leading to Eq. (8). Note that for the case of *distant* chains where $t_\perp \sim \exp(-a_\perp/a_B)$, the correct limiting result $\xi_\perp = a_B$ is recovered.

In contrast, for the tunneling along the chain the soliton mechanism is the winner. Consider first the longitudinal tunneling of a soliton in the absence of impurities. Employing the usual imaginary-time picture, the action for tunneling over a distance $x \gg l_s$ can be estimated as the product of the energy barrier W and the tunneling time $\tau \sim x/u$. Here u, given by

$$u = \left(\frac{C_x}{ma}\right)^{1/2} \sim \frac{e^2}{\kappa \hbar} \frac{1}{\sqrt{r_s}}, \tag{B3}$$

is the sound velocity.[64] The tunneling amplitude is of the order of $\exp(-Wx/\hbar u)$. Using $W \sim e^2/\kappa l_s$, we arrive at the estimate of the localization length as follows:

$$\xi_x^s \sim \frac{l_s}{\sqrt{r_s}} \quad (l = \infty), \tag{B4}$$

where the superscript s stands for "soliton." Clearly, $\xi_x^s \gg \xi_x^q$, so that the soliton mechanism dominates the longitudinal tunneling. To account for the dilute impurities, we should add to the above expression for the action an extra term $(x/l)[\hbar \sqrt{r_s} \ln(l_s/a)]$. Here the factor (x/l) is the average number of impurities on the tunneling path of length x and the expression inside the square brackets is the action cost for compactification of the charge e from the length l_s to length a and spreading it back during the tunneling through each impurity. In this manner, we obtain a corrected expression for ξ_x, which coincides with Eq. (55).

APPENDIX C: DIMENSIONAL ENERGY ESTIMATES FOR THE COLLECTIVE PINNING

In this appendix we use the ideas of collective pinning to derive the growth of elastic distortions in a quasi-1D crystal pinned by strong dilute impurities. We also derive the estimates of the corresponding gain in the pinning energy density.

We start by reformulating the argument leading to Eq. (33) in the language conventional in the literature devoted to collective pinning.[19] To do so we note that since the energy of a given soliton dipole E_s depends on the background elastic displacement field $\bar{u}$, each impurity exerts a force $f = -\partial E_s/\partial \bar{u} \sim W/a$ on the crystal. The long-range variations of $\bar{u}$ appear in response to such random forces. Let $\Delta u(D)$ be a characteristic variation of $\bar{u}$ over a distance D in the transverse direction and let X be a typical distance over which a variation of the same order in the x direction builds up. Our next step is to estimate the total energy E of a volume $V = X \times D \times D$ (relative to the energy of a pristine crystal).

The energy consists of elastic, Coulomb, and pinning parts,

$$E = E^{el} + E^C + E^{pin}. \tag{C1}$$

In its turn, E^{el} is the sum of the longitudinal and transverse terms,

$$E^{el} \sim Y_x \left(\frac{\Delta u}{X}\right)^2 V + Y_\perp \left(\frac{\Delta u}{D}\right)^2 V. \tag{C2}$$

The Coulomb energy is of the order of $\tilde{U}(q_x,q_\perp)\rho^2 V$, where $\tilde{U}(q)=4\pi e^2/\kappa q^2$ is the Coulomb kernel, $q_x=1/X$, $q_\perp=1/D$ are the characteristic wave vectors involved, $\rho=en\partial_x u\sim en\Delta u/X$ is the charge density associated with the londitudinal compression, and $n=1/aa_\perp^2$ is the average electron concentration. Below we show that $D\ll X$, so that $q_\perp\gg q_x$, $\tilde{U}(q)\sim e^2 D^2/\kappa$, and finally,

$$E^C\sim\frac{e^2}{\kappa}\frac{D^4}{X}\left(\frac{\Delta u}{aa_\perp^2}\right)^2. \qquad (C3)$$

The pinning energy can be estimated as $E^{\mathrm{pin}}\sim-\Delta u\Sigma_j f_j$, where $f_j\sim W/a$ is the force exerted on the lattice by jth impurity. The average number of impurities in the volume V is $N_i=NV$ and f_j have random signs; hence, $E^{\mathrm{pin}}\sim-(W/a)\Delta u\sqrt{N_i}$ or

$$E^{\mathrm{pin}}\sim-W\left(\frac{\Delta u}{a}\right)\left(\frac{D}{a_\perp}\right)\left(\frac{X}{l}\right)^{1/2}. \qquad (C4)$$

Combining Eqs. (A13) and (C2)–(C4), we arrive at

$$E=\frac{W}{a}\left(\frac{\Delta u}{a_\perp}\right)^2\left(\alpha X+\frac{D^4}{Xa_\perp^2}\right)-W\left(\frac{\Delta u}{a}\right)\left(\frac{D}{a_\perp}\right)\left(\frac{X}{l}\right)^{1/2}. \qquad (C5)$$

X and Δu can now be found by optimizing E for a fixed D. Not surprisingly, we find that X and D are related by the defining equation (30) of the paraboloid introduced in Sec. V A (for $r_D\sim a_\perp$ case),

$$X\sim\frac{D^2}{a_\perp\sqrt{\alpha}}. \qquad (C6)$$

Such a paraboloid is an invariable feature of the elastic response of the quasi-1D crystal to external forces. What is, surprising, however is that $\Delta u^2\sim(l_s/l)a^2$ is small and does not depend on D, at odds with Eq. (32). The resolution of this contradiction comes from a realization that what $\Delta u(D)$ really represents is the elastic distortion due to the adjustment of the crystal on a single scale D. In fact, there is a hierarchy of smaller scales $D,D/2,D/4,\ldots,r_\perp^{\mathrm{min}}$, on which adjustments are approximately independent. The correct estimate of Δu, Eq. (32), is obtained once we sum over all such scales, $\Delta u^2\sim Ma^2 l_s/l$, where $M\sim\ln(D/r_\perp^{\mathrm{min}})$ is the number of scales. Thereby, we recover Eq. (32) and as an additional benefit, we find the expression for the energy of the collective pinning,

$$E\sim-W\left(\frac{\Delta u}{a}\right)^2\left(\frac{D}{a_\perp}\right)^2. \qquad (C7)$$

Let us define the pinning energy density by $\mathcal{E}_{\mathrm{pin}}=E/XD^2$. Using Eqs. (28), (33), (C6), and (C7) we obtain the estimate of $\mathcal{E}_{\mathrm{pin}}$ at the Larkin scale as given by Eq. (34). As clear from this derivation, both Eqs. (32) and (34) are essentially the lowest-order perturbation theory results. It is generally expected that the growth of Δu^2 with r slows down beyond the Larkin length[65] and that adjustments on larger scales do not lead to any substantial increase in the pinning energy density. In this case, Eq. (34) is the final estimate of $\mathcal{E}_{\mathrm{pin}}$ in the thermodynamics limit.

[1] Yu Lu, *Solitons and Polarons in Conducting Polymers* (World Scientific, Singapore, 1988).

[2] A.J. Heeger, S. Kivelson, J.R. Schrieffer, and W.-P. Su, Rev. Mod. Phys. **60**, 781 (1984).

[3] N.F. Mott and E.A. Davis, *Electronic Processes in Non-Crystalline Materials* 2nd ed. (Clarendon Press, Oxford, 1979).

[4] B.I. Shklovskii and A.L. Efros, *Electronic Properties of Doped Semiconductors* (Springer, New York, 1984).

[5] For review, see M.M. Fogler, in *High Magnetic Fields: Applications in Condensed Matter Physics and Spectroscopy*, edited by C. Berthier, L.P. Levy, and G. Martinez (Springer-Verlag, Berlin, 2002); M.M. Fogler, cond-mat/0111001 (unpublished).

[6] J.M. Tranquada in *Neutron Scattering in Layered Copper-Oxide Superconductors*, edited by A. Furrer (Kluwer, Dordrecht, 1998); J.M. Tranquada in Ref. 12.

[7] R.G. Mani and K.v. Klitzing, Phys. Rev. B **46**, 9877 (1992).

[8] W.A. de Heer, W.S. Basca, A. Chatelain, T. Gerfin, R. Humphrey-Baker, L. Forró, and D. Ugarte, Science **268**, 845 (1995); O. Chauvet, L. Forró, L. Zuppiroli, and W.A. De Heer, Synth. Met. **86**, 2311 (1997).

[9] F.J. Himpsel, K.N. Altmann, R. Bennewitz, J.N. Crain, A. Kirakosian, J.-L. Lin, and J.L. McChesney, J. Phys.: Condens. Matter **13**, 11 097 (2001).

[10] For review, see G. Grüner, *Density Waves in Solids* (Addison-Wesley, New York, 1994); G. Grüner, Rev. Mod. Phys. **60**, 1129 (1988).

[11] *Highly Conducting Quasi-One-Dimensional Organic Crystals*, edited by E. Conwell, Semiconductors and Semimetals Vol. 27 (Academic Press, San Diego, 1988).

[12] For other representative works on the subject, see also in *ECRYS-2002*, Proceedings of An International Workshop on Electronic Crystals, edited by S.A. Brazovskii, N. Kirova, and P. Monceau [J. Phys. IV **12** (2002)].

[13] L.I. Glazman, I.M. Ruzin, and B.I. Shklovskii, Phys. Rev. B **45**, 8454 (1992).

[14] H.J. Schulz, Phys. Rev. Lett. **71**, 1864 (1993).

[15] X.G. Wen, Phys. Rev. B **42**, 6623 (1992); D. Boies, C. Bourbonnais, and A.-M.S. Tremblay, Phys. Rev. Lett. **74**, 968 (1995); E. Arrigoni, Phys. Rev. B **61**, 7909 (2000).

[16] A.O. Gogolin, A.A. Nersesyan, and A.M. Tsvelik, *Bosonization Approach to Strongly Correlated Systems* (Cambridge University Press, Cambridge, 1999).

[17] T. Giamarchi and H.J. Schulz, Phys. Rev. B **37**, 325 (1988), and references therein.

[18] C.L. Kane and M.P.A. Fisher, Phys. Rev. B **46**, 15 233 (1992).

[19] G. Blatter, M.V. Feigel'man, V.B. Geshkenbein, A.I. Larkin, and V.M. Vinokur, Rev. Mod. Phys. **66**, 1125 (1994).

[20] For VRH transport in a model of noninteracting quasi-1D electron system, see E.P. Nakhmedov, V.N. Prigodin, and A.N. Sam-

ukhin, Fiz. Tverd. Tela (Leningrad) **31**, 31 (1989) [Sov. Phys. Solid State **31**, 368 (1989)].

[21] D.J. Bergman, T.M. Rice, and P.A. Lee, Phys. Rev. B **15**, 1706 (1977).

[22] K.B. Efetov and A.I. Larkin, Zh. Eksp. Teor. Fiz. **72**, 2350 (1977) [Sov. Phys. JETP **45**, 1236 (1977)].

[23] A.I. Larkin, Zh. Eksp. Teor. Fiz. **105**, 1793 (1994) [Sov. Phys. JETP **78**, 971 (1994)].

[24] T.M. Rice, A.R. Bishop, J.A. Krumhansl, and S.E. Trullinger, Phys. Rev. Lett. **36**, 432 (1976).

[25] S.A. Brazovskii and N. Kirova, in *Soviet Scientific Reviews*, edited by I.M. Khalatnikov, Physics Reviews Vol. 6 (Harwood, New York, 1984), Sec. A.

[26] In principle, vacancies bound to the acceptors can also be viewed as 2π-phase (anti) solitons (Refs. 24 and 25) of extremely short length $\sim a$, see S. Barisić and I. Batistić, J. Phys. I **50**, 2717 (1989). Likewise, interstitial electrons are 2π-phase solitons. Such microscopic-size solitons remain strongly bound to their impurities and do not play a role in the low-T transport.

[27] S.A. Brazovskii and S.I. Matveenko, Zh. Eksp. Teor. Fiz. **99**, 887 (1991) [Sov. Phys. JETP **72**, 492 (1991)].

[28] A.L. Efros and B.I. Shklovskii, J. Phys. C **8**, L49 (1975).

[29] B.I. Shklovskii and A.L. Efros, in *Electron-Electron Interactions in Disordered Systems*, edited by A.L. Efros and M. Pollak (North-Holland, Amsterdam, 1985).

[30] M.E. Raikh and A.L. Efros, Pis'ma Zh. Eksp. Teor. Fiz. **45**, 225 (1987) [JETP Lett. **45**, 280 (1987)].

[31] T. Nattermann, T. Giamarchi, and P. Le Doussal, Phys. Rev. Lett. **91**, 056603 (2003).

[32] A.I. Larkin and P.A. Lee, Phys. Rev. B **17**, 1596 (1978).

[33] V.K.S. Shante, Phys. Rev. B **16**, 2597 (1977).

[34] S. Rouziere, S. Ravy, J.-P. Pouget, and S. Brazovskii, Phys. Rev. B **62**, 16 231 (2000).

[35] L. Zuppiroli, *Highly Conducting Quasi-One-Dimensional Organic Crystals*, edited by E. Conwell, Semiconductors and Semimetals Vol. 27 (Ref. 11), Ch. 7.

[36] J.M. Benoit, B. Corraze, and O. Chauvet, Phys. Rev. B **65**, 241405 (2002).

[37] C.O. Yoon, M. Reghu, D. Moses, A.J. Heeger, Y. Cao, T.-A. Chen, X. Wu, and R.D. Rieke, Synth. Met. **75**, 229 (1995).

[38] M.J. Rice and J. Bernasconi, Phys. Rev. Lett. **29**, 2597 (1972).

[39] S. Kivelson, Phys. Rev. B **25**, 3798 (1982).

[40] Q. Li, L. Cruz, and P. Phillips, Phys. Rev. B **47**, 1840 (1993).

[41] We were unable to find in literature a derivation of the coefficient C_5 that consistently takes into account the random distribution of rods lengths and their mutual depolarization fields. Our own derivation (Ref. 44) shows that $C_5 = 1/6$ in the limit $r_D \ll a_\perp$, while in the case of interest, $r_D \sim a_\perp$, C_5 should be of the order of unity and may depend on the type of the lattice (square, rectangular, etc.) formed by the chain array.

[42] L.D. Landau and E.M. Lifshitz, *Electrodynamics of Continuous Media*, 2nd ed., by E.M. Lifshitz and L.P. Pitaevskii (Pergamon, New York, 1984).

[43] A.L. Efros, J. Phys. C **9**, 2021 (1976).

[44] M.M. Fogler, S. Teber, and B.I. Shklovskii (unpublished).

[45] For the case $\xi_\perp \to 0$, see Table I in Sec. II.

[46] Similar ideas were investigated earlier by S. Abe, J. Phys. Soc. Jpn. **54**, 3494 (1985); **55**, 1987 (1986); see also J.R. Tucker, W.G. Lyons, and G. Gammie, Phys. Rev. B **38**, 1148 (1988).

[47] M.M. Fogler and D.A. Huse, Phys. Rev. B **62**, 7553 (2000).

[48] S. Brazovskii, J. Phys. I **3**, 2417 (1993).

[49] P.A. Lee, T.M. Rice, and P.W. Anderson, Solid State Commun. **14**, 703 (1974).

[50] L. Zuppiroli, S. Bouffard, K. Bechgaard, B. Hilti, and C.W. Mayer, Phys. Rev. B **22**, 6035 (1980).

[51] G. Mihaly, S. Bouffard, and L. Zuppiroli, IEE Proc., Part I: Solid-State Electron Devices **41**, 1495 (1980).

[52] A. Jànossy, K. Holczer, P.L. Hsieh, C.M. Jackson, and A. Zettl, Solid State Commun. **43**, 507 (1982).

[53] S.N. Artemenko and F. Gleisberg, Phys. Rev. Lett. **75**, 497 (1995).

[54] D. Kuse and H.R. Zeller, Phys. Rev. Lett. **27**, 1060 (1971); **28**, 1452 (1972).

[55] J.F. Thomas, Solid State Commun. **42**, 567 (1982).

[56] S.K. Zhilinskii, M.E. Itkis, I.Yu. Kal'nova, F.Ya. Nad, and V.B. Preobrazhenskii, Zh. Éksp. Teor. Fiz. **85**, 362 (1983) [Sov. Phys. JETP **58**, 211 (1983)].

[57] M.E. Itkis, F.Ya. Nad, and P. Monceau, J. Phys.: Condens. Matter **2**, 8327 (1990).

[58] K. Hosseini, W. Brütting, M. Schwoerer, E. Riedel, S. van Smaalen, K. Biljaković, and D. Staresinić, J. Phys. IV **9**, Pr10-41 (1999).

[59] B. Zawilski, T. Klein, and J. Marcus, Solid State Commun. **124**, 39 (2002).

[60] J. Joo, S.M. Long, J.P. Pouget, E.J. Oh, A.G. MacDiarmid, and A.J. Epstein, Phys. Rev. B **57**, 9567 (1998).

[61] A.N. Aleshin, S.R. Williams, and A.J. Heeger, Synth. Met. **94**, 173 (1997).

[62] M.M. Fogler, cond-mat/0206390 (unpublished).

[63] Our conclusions differ from those of Ref. 53, where an unphysical limit $r_D \ll a_\perp$ is considered.

[64] If the electron-phonon coupling is important, Borh radius a_B and the r_s parameter must be calculated based on the enhanced electron effective mass (Refs. 10 and 49) m_*, i.e., $r_s = e^2 a m_* / 2\hbar^2 \kappa$. Thus, the mass enhancement decreases the sound velocity u and suppresses the tunneling, as may be expected on physical grounds.

[65] Several nonperturbative approaches predict the double-logarithmic dependence, see R. Chitra, T. Giamarchi, and P. Le Doussal, Phys. Rev. B **59**, 4058 (1999), and references therein.